Geol. Mag. **149** (*3*), *2012, pp. 532–550. © Cambridge University Press 2011*
doi:10.1017/S0016756811000902

Evidence of crystallization in residual, Cl–F-rich, agpaitic, trachyphonolitic magmas and primitive Mg-rich basalt–trachyphonolite interaction in the lava domes of the Phlegrean Fields (Italy)

LEONE MELLUSO*†, ROBERTO DE' GENNARO‡, LORENZO FEDELE*, LUIGI FRANCIOSI* & VINCENZO MORRA*

*Dipartimento di Scienze della Terra, Università di Napoli Federico II, via Mezzocannone 8, 80134 Napoli, Italy
‡Centro Interdipartimentale Servizi per Analisi Geomineralogiche (CISAG), Università di Napoli Federico II, via Mezzocannone 8, 80134 Napoli, Italy

(*Received* 11 May 2011; *accepted* 19 July 2011; *first published online* 1 November 2011)

Abstract – The lava domes in the northwestern (Cuma), northern (Punta Marmolite) and central (Accademia) parts of the Phlegrean Fields are the subject of this study. The Cuma and Punta Marmolite trachyphonolitic lava domes are among the oldest Phlegrean products cropping out. The Cuma rocks have an agpaitic groundmass, with early alkali feldspar, Fe-rich clinopyroxene, Fe-edenite and sodalite and late rosenbuschite, fluorite, baddeleyite, pyrochlore, britholite, monazite, aegirine (often Zr-rich) and exceptionally Fe–Mn-rich olivine. The bulk-rock compositions at Cuma have some of the highest concentrations of Zn, Mn, Zr, Nb, Th, U and lanthanides among the Phlegrean Fields rocks, and some of the lowest MgO, P_2O_5, Sr, Eu and Ba. The Punta Marmolite dome is chemically less evolved, and lacks characteristic agpaitic minerals, but features alkali feldspar, sodalite, nepheline and relatively Na-poor, Fe-rich hedenbergite, with rare Ca-rich plagioclase xenocryst cores. The Accademia dome, belonging to the recent activity, is latitic to trachytic in composition, has highly forsteritic olivine (with chromiferous spinel inclusions), calcic plagioclase and Mg-rich diopside (± phlogopite) xenocrysts in an evolved host rock (with phenocrysts and microlites of alkali feldspar, Fe-rich clinopyroxene, Fe-rich amphibole, magnetite, Fe-rich olivine and accessory baddeleyite, zirconolite and fluorite). There is clear evidence of open-system magma crystallization in the form of interaction between a crystallizing, primitive shoshonitic basalt in a reservoir already filled by rather evolved trachytic magma. The magmatic evolution towards the evolved compositions is dominated by crystallization of more and more Na-rich alkali feldspar in a Cl-, F-rich and relatively H_2O-poor environment. Input of mafic magma is evident in many trachytic eruptions of the Phlegrean Fields and even in the products of the Campanian Ignimbrite, but eruptions having mineral assemblages rich in xenocryst phases as well as eruptions virtually free of mafic magma input are also frequently observed throughout the history. This suggests a variable pattern of open- and closed-system crystallization, which may or may not be linked to explosive activity, and that can be caused by intermittent supply of basaltic magma from depth.

Keywords: trachyphonolites, agpaitic rocks, rosenbuschite, fayalite-tephroite, xenocrysts, Phlegrean Fields feeder system, Italy.

1. Introduction, geological setting and sampling sites

The Phlegrean Fields (Campi Flegrei) is a volcanic area that includes the urban area of Naples and its western outskirts (Fig. 1), and is part of the Campanian district, which includes Ischia, Procida and Somma-Vesuvius. The Phlegrean Fields are characterized by a great number of explosive eruptions, the most powerful of which produced the Campanian Ignimbrite (CI; ∼ 39 ka; De Vivo *et al*. 2001; Fedele *et al*. 2008) and the Neapolitan Yellow Tuff (NYT; ∼ 15 ka; Deino *et al*. 2004), the two most important events in the volcanic history of the area which determined the development of a nested caldera (see Perrotta *et al*. 2006). The CI and NYT deposits are the main chronostratigraphic markers for the reconstruction of Phlegrean activity, which can be broadly subdivided into three periods: (1) pre-CI; (2) between CI and NYT and (3) post-NYT. The post-NYT 'recent' activity has been commonly subdivided into three epochs of active volcanism separated by quiescent intervals (Orsi *et al*. 2009 and references therein), although there is evidence that the subdivision is more complex (Insinga *et al*. 2006; Fedele *et al*. 2011). The Phlegrean Fields are potentially active, as testified by the last eruption of Monte Nuovo (AD 1538), the 1970–72 and 1982–84 bradyseismic episodes, and intense fumarolic activity.

Phlegrean rock compositions range from shoshonitic basalt through latite, to trachyte, trachyphonolite and phonolite, with the chemically evolved products predominating. The least-evolved compositions have geochemical and isotopic signatures commonly

†Author for correspondence: melluso@unina.it

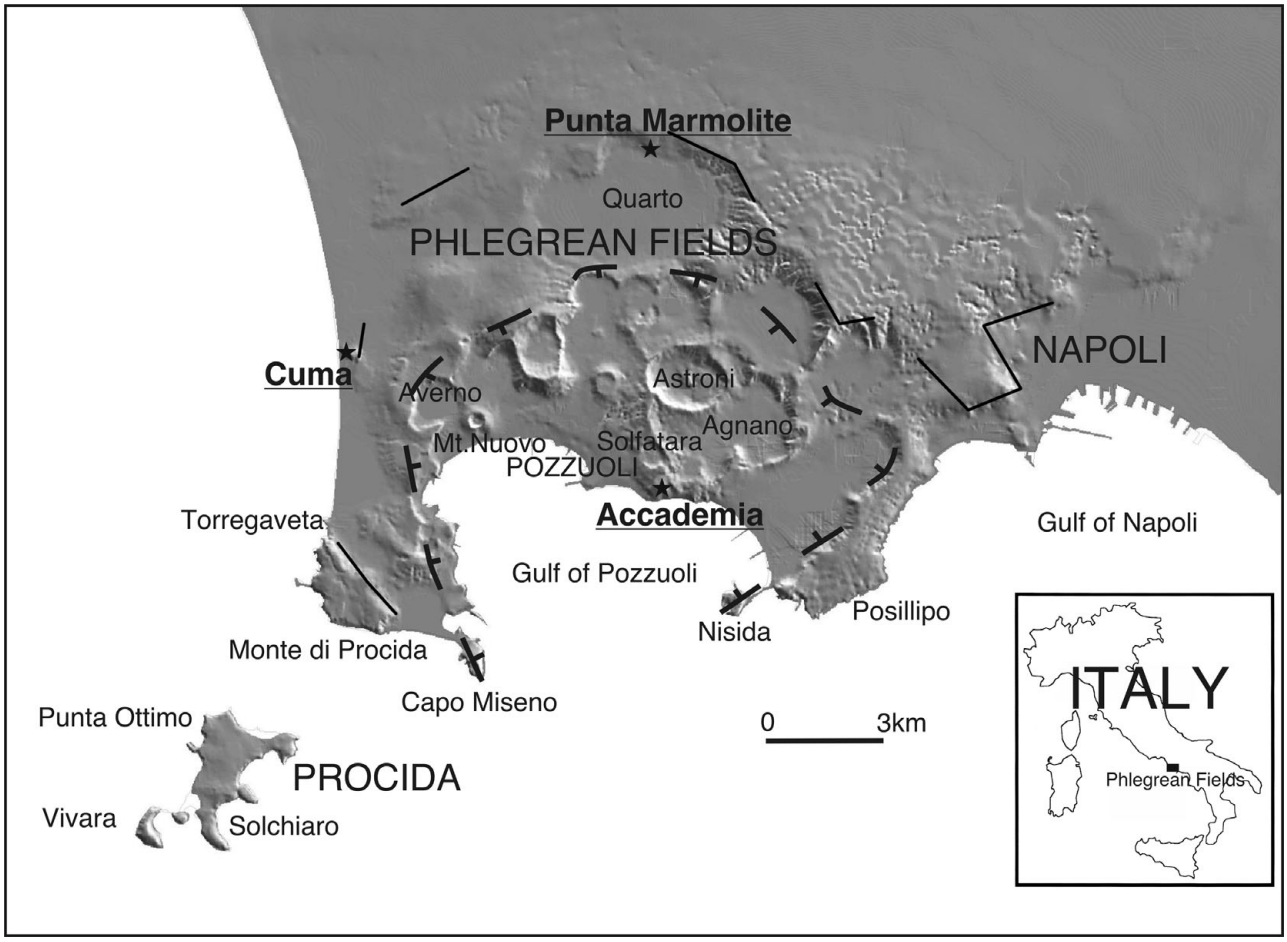

Figure 1. Sketch map of Phlegrean Fields, with main localities and sampling sites (image after Vilardo *et al*. 2001).

interpreted as indicative of subduction-related magmatism, generated by melting mantle metasomatized by fluids and melts from the still seismically active subducting slab (e.g. high LREE/HREE and LILE/HFSE ratios and Sr-, Nd-, Pb- and B-isotopic signature; LREE = light lanthanides; HREE = heavy lanthanides; LILE = large-ion lithophile elements; HFSE = high-field-strength elements; e.g. Beccaluva, Di Girolamo & Serri, 1991; Beccaluva *et al*. 2002; D'Antonio *et al*. 2007; D'Antonio, Civetta & Di Girolamo, 1999; Avanzinelli *et al*. 2009).

The evolution of Phlegrean magmas is generally thought to be driven mainly by fractional crystallization processes (e.g. Di Girolamo, 1970; Villemant, 1988; Melluso *et al*. 1995; Fowler *et al*. 2007; Fedele *et al*. 2008, 2009; D'Antonio, 2011), although open-system processes (crustal contamination, magma mixing/mingling) also seem to have been active, as testified by several lines of evidence, including (a) the occasional presence of xenocryst phases (e.g. Beccaluva *et al*. 1990; Civetta *et al*. 1997; Fedele *et al*. 2008, 2009) and (b) significant isotopic variability in the juvenile products (e.g. Civetta *et al*. 1997; D'Antonio *et al*. 1999, 2007; Pappalardo *et al*. 1999, 2002; Pabst *et al*. 2008; Di Renzo *et al*. 2011).

The samples of the present study belong to some of the relatively limited effusive products of the Phlegrean Fields (mainly explosive) activity: the lava domes of Cuma, Punta Marmolite and Accademia (also known as Mt Olibano). The Cuma and Punta Marmolite domes, with unspiked K–Ar ages of 37 and 47 ka, respectively (Cassignol & Gillot, 1982), have been emplaced on sectors involved in the caldera collapse related to the CI eruption, whereas the Accademia dome was emplaced at *c*. 3.9 ka (K–Ar; Di Girolamo *et al*. 1984) in the central part of the Phlegrean volcanic area, close to the Solfatara crater, the Agnano plain and in front of the roughly coeval Nisida tuff cone (3.9 ka Ar–Ar; Fedele *et al*. 2011).

This paper is the first report of the occurrence and compositional range for most minerals in Phlegrean Fields magmatic rocks. Therefore, this study provides information on the complete crystallization history of the Phlegrean Fields magmas to date, and helps to shed light on the processes that generate agpaitic rocks in silica-undersaturated trachytic systems in Italy and elsewhere. Moreover, the occurrence of chromiferous spinel, forsterite-rich olivine and other high-temperature minerals in the Accademia latite is also another undescribed and intriguing feature of the plumbing system.

The detailed study of the mineral assemblages and the mineral compositions of the almost unknown lava domes of the Phlegrean Fields (see the very few

https://doi.org/10.1017/S0016756811000902 Published online by Cambridge University Press

data reported by Di Girolamo *et al*. 1984; Rosi & Sbrana, 1987; D'Antonio *et al*. 1999; Pappalardo *et al*. 1999; Isaia, Marianelli & Sbrana, 2009; Morra *et al*. 2010) indicates a very prolonged crystallization history, unlike the Phlegrean pyroclastic rocks, and provides useful information on the following topics: (a) closed-system crystallization of highly evolved silica-undersaturated trachytic-trachyphonolitic compositions; (b) recharge in shallow magma reservoirs, with recycling of xenocrysts derived by distinct, often very magnesian, magma batches; (c) relevance for the Phlegrean Fields feeder system.

The magmatic assemblages of peralkaline undersaturated rocks have been studied in the classic settings of the Oslo rift in Norway and the Gardar Province of south Greenland (Sørensen, 1974; Larsen & Sørensen, 1987; Andersen *et al*. 2010 and references therein), and are of economic interest: studies on mineral assemblages and evolution trends in peralkaline oversaturated rocks are far more abundant (see White, Ren & Parker, 2005; Ronga *et al*. 2010; Macdonald *et al*. 2011 and references therein). Our study adds a piece of knowledge on the final stages of crystallization in silica-undersaturated magmatic systems, where the main volatiles involved are Cl and F, as well as H_2O.

2. Analytical techniques

Samples of the three lava domes, together with scorias of the Nisida tuff cone (Fedele *et al*. 2011) were collected, cut with a saw and crushed in a jaw crusher. Powders were produced in a low-blank agate mortar from clean chips first washed in distilled water. Major and trace elements were analysed by ICP-MS (inductively coupled plasma mass spectrometry) at ACTLABS, Ancaster, Ontario (see www.actlabs.com for details of the analytical procedures and Table 1 for analyses of reference standards). A few trace elements were analysed by XRF (X-ray fluorescence) at University of Napoli Federico II using pressed powder pellets and an Axios Panalytical instrument (see Ronga *et al*. 2010 for details). Some 950 mineral compositions were obtained with Energy Dispersive Spectrometry at CISAG, University of Napoli Federico II, utilizing an Oxford Instruments Microanalysis Unit, equipped with an INCA X-act detector and a JEOL JSM-5310 microscope operating at a 15 kV primary beam voltage, 50–100 μA filament current, variable spot size and 50 s net acquisition time. Measurements were done with an INCA X-stream pulse processor. The following standards were used for calibration: diopside (Mg), wollastonite (Ca), anorthoclase (Al, Si), albite (Na), rutile (Ti), almandine (Fe), Cr_2O_3 (Cr), rhodonite (Mn), orthoclase (K), apatite (P), fluorite (F), barite (Ba), strontianite (Sr), zircon (Zr, Hf), ilmenite (Nb), synthetic Smithsonian orthophosphates (La, Ce, Nd, Sm, Y), pure vanadium (V), Corning glass (Th and U), sphalerite (S, Zn), sodium chloride (Cl) and pollucite (Cs). Backscattered electron (BSE) images were obtained with the same instrument (see Melluso, Conticelli & de'Gennaro, 2010 and Melluso, de'Gennaro & Rocco, 2010 for details).

3. Petrography and bulk-rock compositions

The samples of the massive facies of the Cuma dome (Fig. 2a–d; samples DC2, DC3) are porphyritic, with sparse phenocrysts of zoned sanidine, set in a fine-grained fluidal holocrystalline mesostasis made of sanidine and sodalite, with clinopyroxene, amphibole, olivine, oxides, fluorite, apatite and other phases. Plagioclase is absent. Yellow olivine is common as microlite and encloses feldspar, apatite and magnetite.

The samples of the massive facies of the Punta Marmolite dome (Fig. 2e, f; samples DPM2, DPM3) are weakly porphyritic, with sanidine (sometimes mantling plagioclase) and sodalite phenocrysts, rare subhedral nepheline, magnetite and clinopyroxene microphenocrysts in a holocrystalline, strongly fluidal groundmass with the same minerals and accessories, among which apatite-britholite, fluorite and baddeleyite are the most abundant.

The samples of the Accademia dome (Fig. 2g–k) have at least two different facies. Samples from the front of the 'Cava Regia' quarry (samples OL1, OL2) have phenocrysts of plagioclase, colourless to pale-green clinopyroxene, sanidine, resorbed phlogopite and olivine with spinel inclusions, often arranged in glomeroporphyritic clusters of clinopyroxene, plagioclase and phlogopite, or plagioclase and sanidine, and set in a groundmass of sanidine, Fe-rich olivine, clinopyroxene and magnetite. Baddeleyite and fluorite are very frequent accessory phases. Plagioclase is frequently and abruptly mantled by sanidine (never the reverse), and crystallized earlier than, or contemporaneously with, Mg-clinopyroxene. The other facies, represented by very large blocks of several tens of cubic metres at the base of the quarry and along the 'La Pietra' coastline (sample DAF1) and in the surrounding areas, is devoid of olivine phenocrysts, has sanidine phenocrysts, with plagioclase inclusions, small amounts of green-brown amphibole surrounding greenish clinopyroxene (Fig. 2j), and a more interstitial green clinopyroxene, with microlites of yellow olivine, found interstitial to sanidine and in the groundmass (Fig. 2g)

The Cuma samples are trachyphonolites, the Punta Marmolite samples are trachytes and trachyphonolites, and the Accademia samples are latites and trachytes, according to the R_1–R_2 classification scheme (Fig. 3a). Major oxides have mild compositional ranges: SiO_2 ranges from 56.7 to 60.7 wt %, MgO ranges from 0.27 to 2 wt %, CaO from 1.7 to 4.6 wt % and Fe_2O_{3t} from 3.8 to 4.9 wt %. The increasing Na_2O/K_2O from Accademia ($Na_2O/K_2O = 0.42$–0.51), through the Punta Marmolite ($Na_2O/K_2O = 0.73$) to Cuma ($Na_2O/K_2O = 1.07$) rocks indicates that the degree of magmatic evolution is accompanied by an increasing sodic character. The Cuma sample reaches 0.84 wt % Cl, whereas the Punta Marmolite sample has Cl = 0.37 wt % and F = 0.04 wt % (Table 1).

https://doi.org/10.1017/S0016756811000902 Published online by Cambridge University Press

Table 1. Major oxides (in wt %), F and Cl (in wt %), trace elements (in ppm) and other parameters for whole-rock samples from the Cuma, Punta Marmolite and Accademia lava domes and for two samples from the Nisida tuff cone.

	Cuma		Punta Marmolite		Accademia			Nisida		measured	certified
	DC3	DC2	DPM2	DPM3	DAF1	OL1	OL2	NIS2	NIS3	W-2a	W-2a
SiO_2	59.15	60.68	59.21	58.89	59.83	58.53	59.70	58.35	56.70	52.22	52.40
TiO_2	0.44	0.44	0.40	0.41	0.47	0.57	0.54	0.49	0.54	1.07	1.06
Al_2O_3	18.59	18.96	18.36	18.66	18.20	17.37	17.83	18.29	17.88	15.02	15.40
Fe_2O_3(t)	3.82	3.76	3.69	3.71	4.02	4.89	4.53	4.33	4.90	10.77	10.70
MnO	0.29	0.29	0.21	0.21	0.13	0.13	0.13	0.13	0.12	0.17	0.16
MgO	0.29	0.27	0.40	0.40	0.77	1.96	1.52	0.96	1.46	6.38	6.37
CaO	1.76	1.66	2.06	2.03	3.00	4.61	3.85	3.34	4.48	11.02	10.90
Na_2O	6.73	7.02	4.95	5.55	3.89	3.49	3.39	4.12	4.86	2.22	2.14
K_2O	6.29	6.56	7.93	7.64	8.19	6.85	8.01	7.73	5.65	0.61	0.63
P_2O_5	0.04	0.06	0.07	0.08	0.18	0.27	0.22	0.21	0.32	0.14	0.13
LOI	1.56	1.12	2.59	1.79	0.47	0.35	0.82	1.25	2.71		
Total	98.93	100.80	99.88	99.37	99.13	99.02	100.50	99.20	99.63		
F wt %			0.04							0.02	0.02
Cl wt %	0.84		0.37								
Be	33	30	19	18	13	11	12	11	9	< 1	1.30
Sc	1	2	1	2	3	9	7	3	4	35	36
V	8	9	13	18	70	108	99	85	116	275	262
Cr	bdl	bdl	bdl	bdl	bdl	40	20	bdl	bdl	90	92
Co	1	1	1	1	5	10	7	6	7	44	43
Ni	bdl	bdl	bdl	bdl	bdl	bdl	bdl	bdl	bdl	70	70
Cu	40	bdl	bdl	bdl	10	20	bdl	10	20	120	110
Zn	190	170	130	130	80	70	60	80	60	90	80
Ga	27	28	22	22	20	19	18	19	17	19	17
Ge	2	2	2	2	2	2	1	1	1	2.0	1.0
As	28	9	30	17	9	14	33	16	13	< 5	1.2
Rb	449	478	343	419	374	289	201	211	150	20.0	21.0
Sr	10	8	54	33	423	521	477	686	982	193.0	190.0
Y	95	79	52	48	32	30	32	29	26	20.0	24.0
Zr	963	1040	547	610	422	365	390	339	270	84.0	94.0
Nb	167	174	100	105	73	56	53	52	41	7.0	7.9
Mo	4	5	bdl	4	5	4	5	3	3	< 2	0.60
Ag	2.6	4	3.4	2	2	2	2	2	1	< 0.5	0.05
Sn	17	14	8	9	6	bdl	bdl	bdl	bdl	bdl	bdl
Sb	2.5	1.6	1.9	1.9	1.3	bdl	bdl	bdl	bdl	1.2	0.8
Cs	25	35	22	32	20	25	19	21	18	0.9	1.0
Ba	39	5	10	12	408	730	616	1049	1780	167	182
La	174.0	208.0	122.0	136.0	97.2	86.4	79.5	79.5	68.6	11.0	10.0
Ce	329.0	319.0	207.0	242.0	175.0	156.0	141.0	139.0	125.0	23.0	23.0
Pr	35.4	38.4	22.9	25.5	18.7	16.5	14.9	14.7	13.1		
Nd	120.0	113.0	75.4	77.1	57.7	56.6	51.5	49.2	44.9	12.00	13.00
Sm	21.3	19.4	13.0	13.3	10.3	10.3	9.3	8.7	7.9	3.00	3.00
Eu	1.4	1.2	1.7	1.7	2.0	2.1	1.9	2.0	2.0	1.02	1.00
Gd	16.4	14.4	9.7	9.9	7.2	7.7	7.1	6.5	5.9		
Tb	2.7	2.4	1.5	1.5	1.1	1.1	1.0	0.9	0.8	0.60	0.63
Dy	16.8	13.5	8.2	8.7	5.9	5.8	5.5	5.0	4.4	3.60	3.60
Ho	3.5	2.6	1.5	1.7	1.1	1.1	1.1	1.0	0.8	0.80	0.76
Er	10.6	7.8	4.6	4.9	3.2	3.1	3.0	2.7	2.3	2.30	2.50
Tm	1.66	1.19	0.72	0.74	0.48	0.47	0.45	0.4	0.33	0.35	0.38
Yb	11.0	8.2	4.9	4.9	3.3	3.0	3.0	2.7	2.2	2.10	2.10
Lu	1.70	1.31	0.81	0.80	0.52	0.50	0.48	0.43	0.35	0.31	0.33
Hf	19.8	23.1	11.3	13.1	10.4	8.7	8.5	7.3	5.7	2.50	2.60
Ta	10.2	9.7	5.7	5.8	3.7	2.9	2.8	2.7	2.0	0.50	0.50
W	16	9	5	7	10	8	6	3	3	< 1	0.30
Tl	0.3	0.9	0.9	0.3	0.5	0.6	0.2	0.6	0.5	0.10	0.20
Pb	69	83	61	67	64	49	44	50	54	9.00	9.30
Th	84.8	78.3	49.9	47.2	40.2	34.5	32.4	30.3	23.1	2.40	2.40
U	22.1	29.0	15.5	18.4	14.1	11.0	9.0	9.7	7.7	0.50	0.53
R_1	−27	−90	230	63	577	921	773	496	594		
R_2	567	563	600	603	716	931	837	764	902		
Mg no.	15	14	20	20	31	48	44	34	41		
AI	0.96	0.98	0.91	0.93	0.84	0.76	0.80	0.83	0.79		
Eu/Eu*	0.22	0.22	0.45	0.46	0.70	0.70	0.70	0.79	0.89		

Loss on ignition (LOI, in wt %) was determined by standard gravimetric techniques. The analyses of reference standard W-2a are reported for comparison. $R_1 = 1000(6Ca + 2Mg + Al)$; $R_2 = 1000(4Si - 11(Na + K) - 2(Fe + Ti))$; $Eu/Eu^* = Eu_N/(Sm_N Gd_N)^{1/2}$ (the subscript N means chondrite-normalized; chondrite of Boynton, 1984); AI = molar $(Na_2O + K_2O)/Al_2O_3$; Mg no. = molar $MgO^*100/(MgO + FeO)$, with $Fe_2O_3/FeO = 0.2$. bdl – below detection limit.

https://doi.org/10.1017/S0016756811000902 Published online by Cambridge University Press

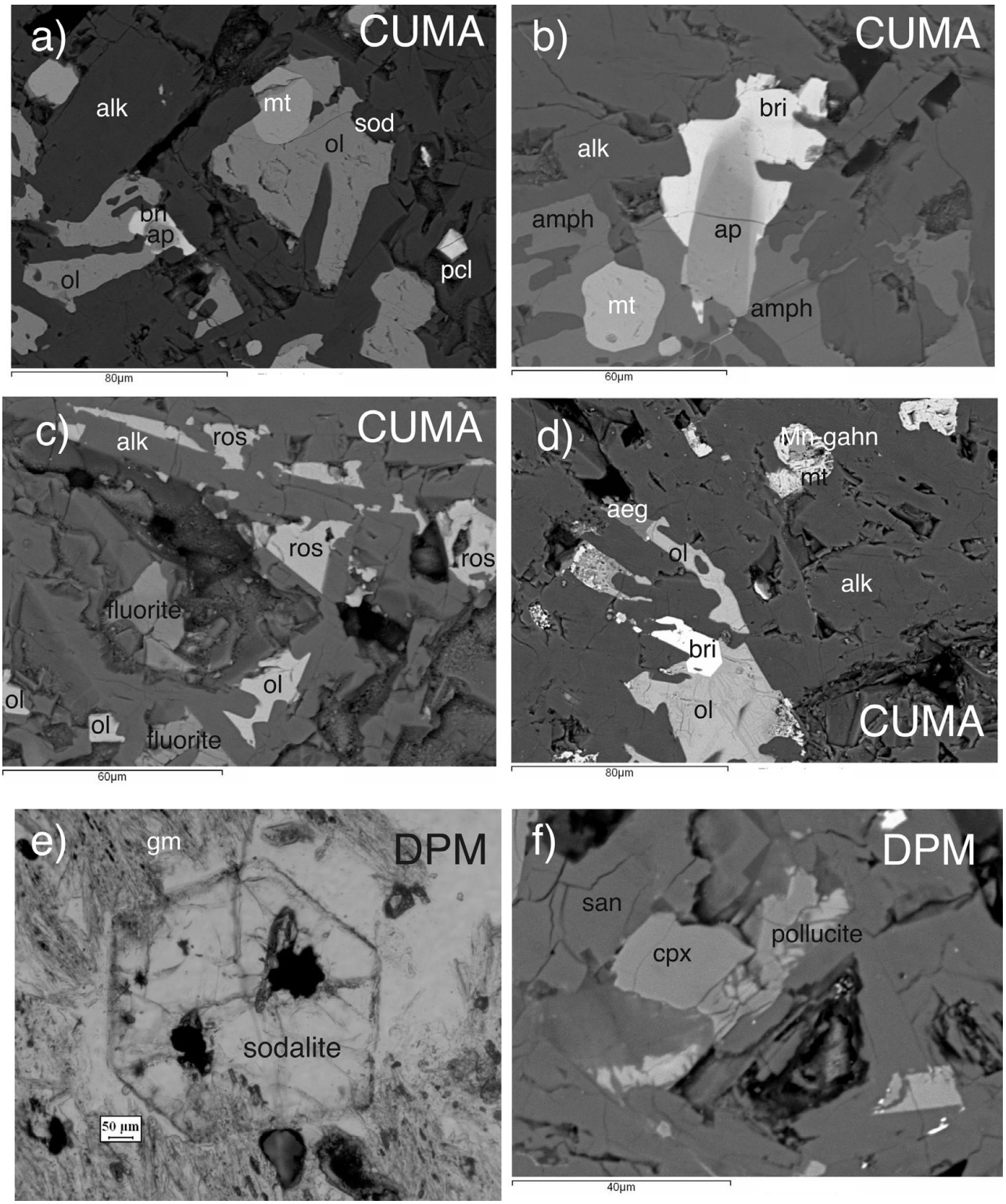

Figure 2. Typical petrographic features of the analysed samples as seen with a polarizing microscope or backscattered electron images (BSE): (a) Cuma dome, BSE: idiomorphic sanidine (alk), magnetite (mt), sodalite (sod) and zoned apatite/britholite (ap, bri) in a poikilitic olivine (ol) and accessory pyrochlore (pcl); (b) Cuma dome, BSE: strongly zoned apatite/britholite, magnetite and alkali feldspar included in poikilitic amphibole (amph); (c) Cuma dome, BSE: poikilitic rosenbuschite (ros), fluorite, olivine (ol) and idiomorphic anorthoclase (alk) in the groundmass; (d) Cuma dome, BSE: idiomorphic britholite, sanidine in poikilitic olivine and late aegirine (aeg); magnetite has a core of gahnite (Mn-gahn); (e) Punta Marmolite dome, parallel nicols: sodalite microphenocryst in a fluidal groundmass (gm); (f) Punta Marmolite dome, BSE: pollucite microlites with sanidine (san) and clinopyroxene (cpx).

The Cuma samples have an agpaitic index (AI, molar $(Na_2O + K_2O)/Al_2O_3$) of 0.96–0.98, while Punta Marmolite and Accademia samples have an AI of 0.91–0.93 and 0.76–0.84, respectively. The Cuma bulk-rock compositions reach among the highest concentrations of Mn (0.29 wt % MnO), Zn (170 ppm), Rb (480 ppm), Zr (1040 ppm) and Nb (174 ppm) reported for the Phlegrean rocks (see Fig. 3b). These values are coupled

https://doi.org/10.1017/S0016756811000902 Published online by Cambridge University Press

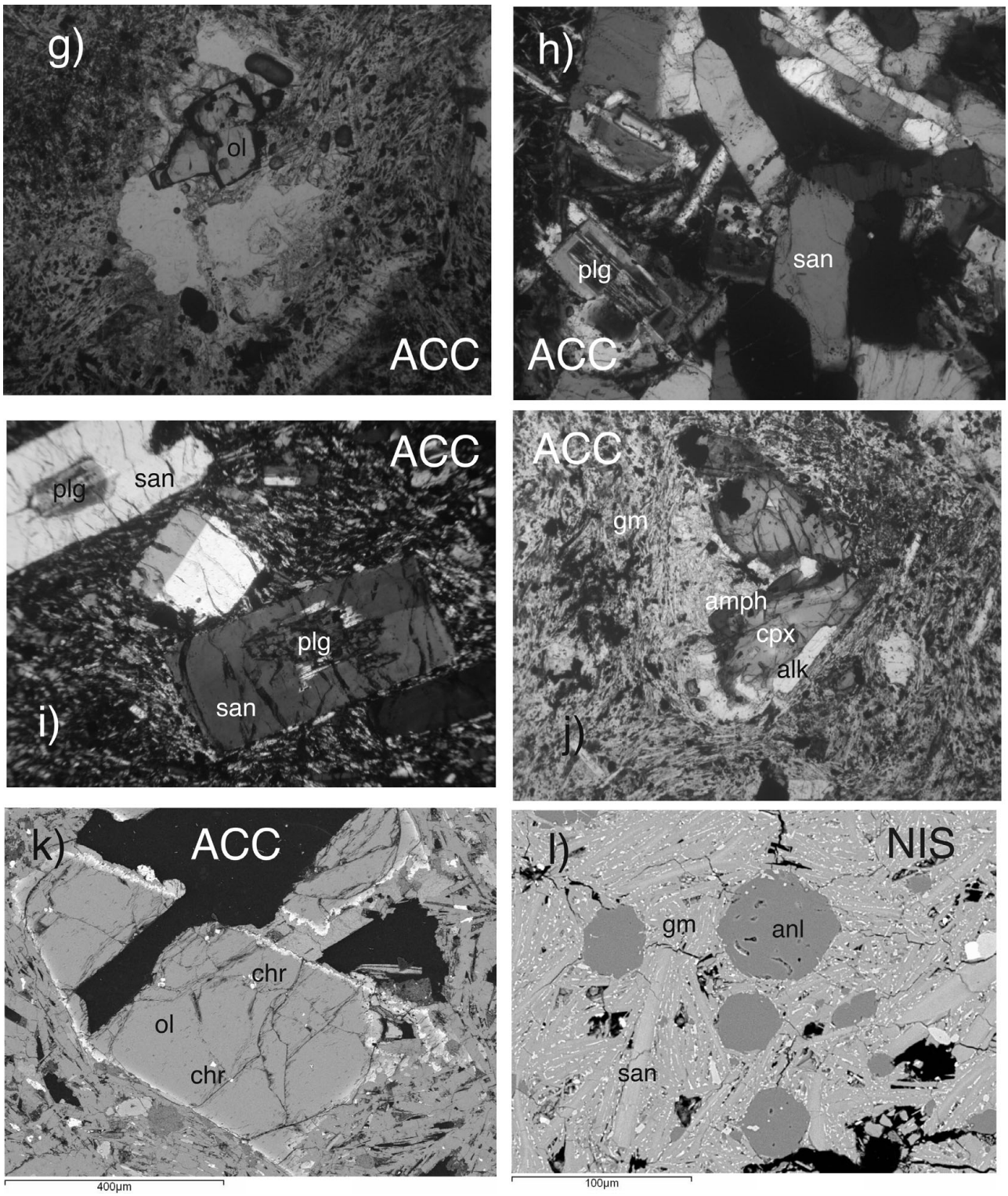

Figure 2. (Continued) (g) Accademia dome, parallel nicols: groundmass fayalite (ol), sanidine and sodalite; (h) Accademia dome, crossed nicols: glomeroporphyritic cluster of sanidine with cores of highly Ca-rich plagioclase (plg); (i) Accademia, crossed nicols: the same feature with sparse phenocrysts; (j) Accademia dome, parallel nicols: clinopyroxene with amphibole rims and inclusions of sanidine (alk) and magnetite; (k) Accademia dome, BSE: idiomorphic, zoned olivine with high-Mg core, high-Fe rims (bright) and chromite inclusions (chr); (l) Nisida tuff cone, BSE: idiomorphic sanidine (san), with bright, Ba–Sr-rich cores, included in idiomorphic analcime (anl), likely former sodalite. gm – groundmass.

with very low MgO (0.27 wt %), P_2O_5 (0.06 wt %), Sr and Ba (both < 10 ppm). Cr and Ni contents are below the detection limits in the Cuma and Punta Marmolite samples, whereas Cr concentration reaches 20–40 ppm in samples OL1 and OL2. Compositional zoning is observed at the Accademia dome, with the samples from the 'Cava Regia' being slightly more mafic with respect to lava blocks from the outskirts of the dome (Table 1).

Total lanthanide (ΣREE) concentrations of the Cuma dome reach about 750 ppm, and are coupled with

https://doi.org/10.1017/S0016756811000902 Published online by Cambridge University Press

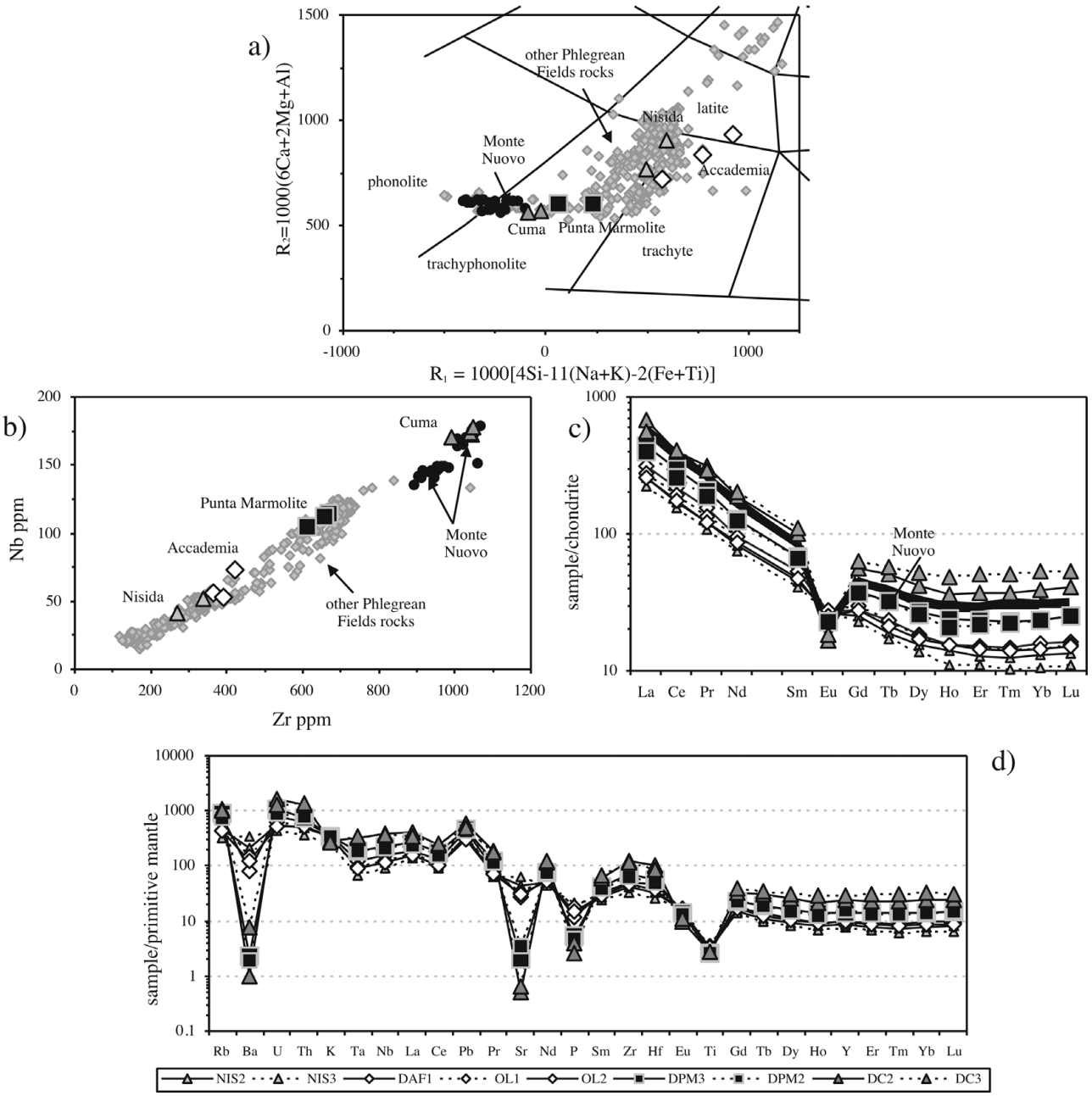

Figure 3. (a) R_1–R_2 classification diagram of the Phlegrean Fields volcanic rocks (after De La Roche *et al*. 1980) with the samples from this study and literature data from D'Antonio *et al*. (1999), Pappalardo *et al*. (2002) and Fedele *et al*. (2008); (b) Zr–Nb diagram with the Phlegrean Fields rock compositions and the samples of this study; the Monte Nuovo analyses are taken from Pappalardo *et al*. (2002) and D'Oriano *et al*. (2005); (c) Lanthanide chondrite-normalized diagrams: the Monte Nuovo lanthanide compositions are taken from D'Oriano *et al*. (2005). Normalization values of Boynton (1984); (d) mantle-normalized multi-element patterns. Normalization values of Lyubetskaya & Korenaga (2007).

the deepest Eu troughs (Eu/Eu* = 0.22; Table 1). At Punta Marmolite, ΣREE is 530 ppm, with a slightly less pronounced Eu trough (Eu/Eu* = 0.46). The samples of the Accademia dome have ΣREE = 320–384 ppm and moderate Eu troughs (Eu/Eu* = 0.70). Worth noting is the parallel shape of the chondrite-normalized patterns (Fig. 3c), with the exception of Eu. On multielemental mantle-normalized diagrams (Fig. 3d), we note that, apart from the similar pattern of all the samples, including those of the Nisida juvenile samples (data in Table 1), the patterns are characterized by very small Ta and Nb troughs, a more marked trough at Ti, peaks at Pb and increasing element abundances towards the rocks of the Cuma dome. The relative concentrations of P, Ba, Sr and Eu decrease towards the most evolved rocks, whereas the Ti, K and Pb abundances are roughly constant.

4. Mineral compositions

4.a. Clinopyroxene and aenigmatite

Clinopyroxene in the Cuma samples ranges continuously from Fe-rich diopside (salite; $Ca_{48}Mg_{30}Fe_{22}$, end-members in atoms %) to almost pure aegirine

https://doi.org/10.1017/S0016756811000902 Published online by Cambridge University Press

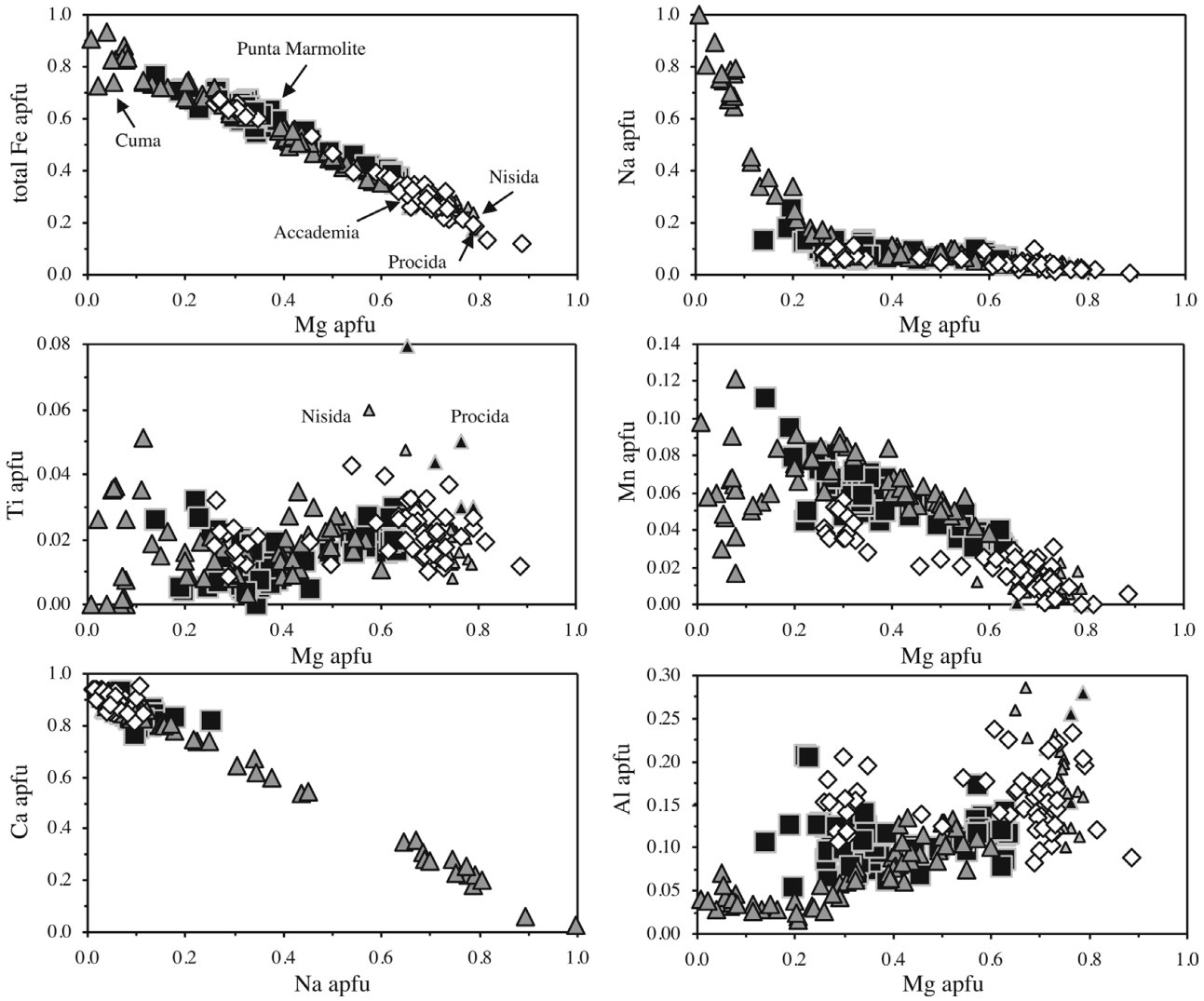

Figure 4. Binary diagrams with analysed clinopyroxene compositions (elements in apfu, atoms for 6 oxygens and 4 cations). The pyroxenes of Nisida and Procida (small triangles) are authors' unpublished data. Note that the marked increase in the aegirine component occurs only at low Mg contents. This corresponds also to a scattered increase in Ti and to the lowest Al contents. The tight correlation between Mg and total Fe suggests that Mg→Fe (regardless of the oxidation state) is the main substitution in the M2 site, and that Fe^{2+} and Fe^{3+} cannot be treated as different cations.

($Na_2O = 13.3$ wt %; $CaO = 0.7$ wt %), the latter present interstitially and occasionally with Zr-rich compositions (up to 3.1 wt % ZrO_2; Table S1 in the online Appendix at http://www.journals.cambridge.org/geo). In the Punta Marmolite samples, clinopyroxene ranges from diopside (salite; $Ca_{45}Mg_{34}Fe_{21}$) to Na-rich hedenbergite (ferrosalite; $Ca_{45}Mg_{11}Fe_{44}$; $Na_2O = 3.3$ wt %). In the Accademia samples, clinopyroxene ranges from Mg-rich diopside ($Ca_{48}Mg_{45}Fe_7$) to hedenbergite ($Ca_{48}Mg_{19-14}Fe_{34-38}$; Na_2O up to 1.45 wt %), showing evident bimodal distribution (Fig. 4). The compositional variation, which covers the complete spectrum from Mg- to Fe-rich compositions, and therefore is thought to be representative of the whole Phlegrean magmatic system, indicates decreasing Al and increasing Fe with decreasing Mg. Ti broadly behaves as Al, with the exception of the most Na-rich pyroxenes, where variable amounts of Ti-rich, Ca–Al-free molecules (such as $NaTi_{0.5}Fe_{0.5}Si_2O_6$ and, for Zr, $NaZr_{0.5}Fe_{0.5}Si_2O_6$) can be sporadically present. Na gently increases to the most Fe-rich compositions and then abruptly reaches pure aegirine compositions in the Cuma samples, whereas Mn increases with Fe, and then decreases in Fe-rich crystals from Cuma (a likely effect of co-crystallization of Mn-olivine and Mn-oxides, see below).

Rare interstitial crystals of aenigmatite ($Na_2Fe_5TiSi_6O_{20}$) have been found in the Cuma dome. The compositions have relatively high Mn (1.8–2.6 wt % MnO; Table S1), higher than the type aenigmatites from Pantelleria (< 1.5 wt % MnO; see White, Ren & Parker, 2005 for reference compositions).

4.b. Feldspar

Low-Ca sodic sanidine-anorthoclase ($Ca_{1-5}Na_{45-63}K_{55-32}$, end-members in atoms %) is the main feldspar of the Cuma dome, with the

https://doi.org/10.1017/S0016756811000902 Published online by Cambridge University Press

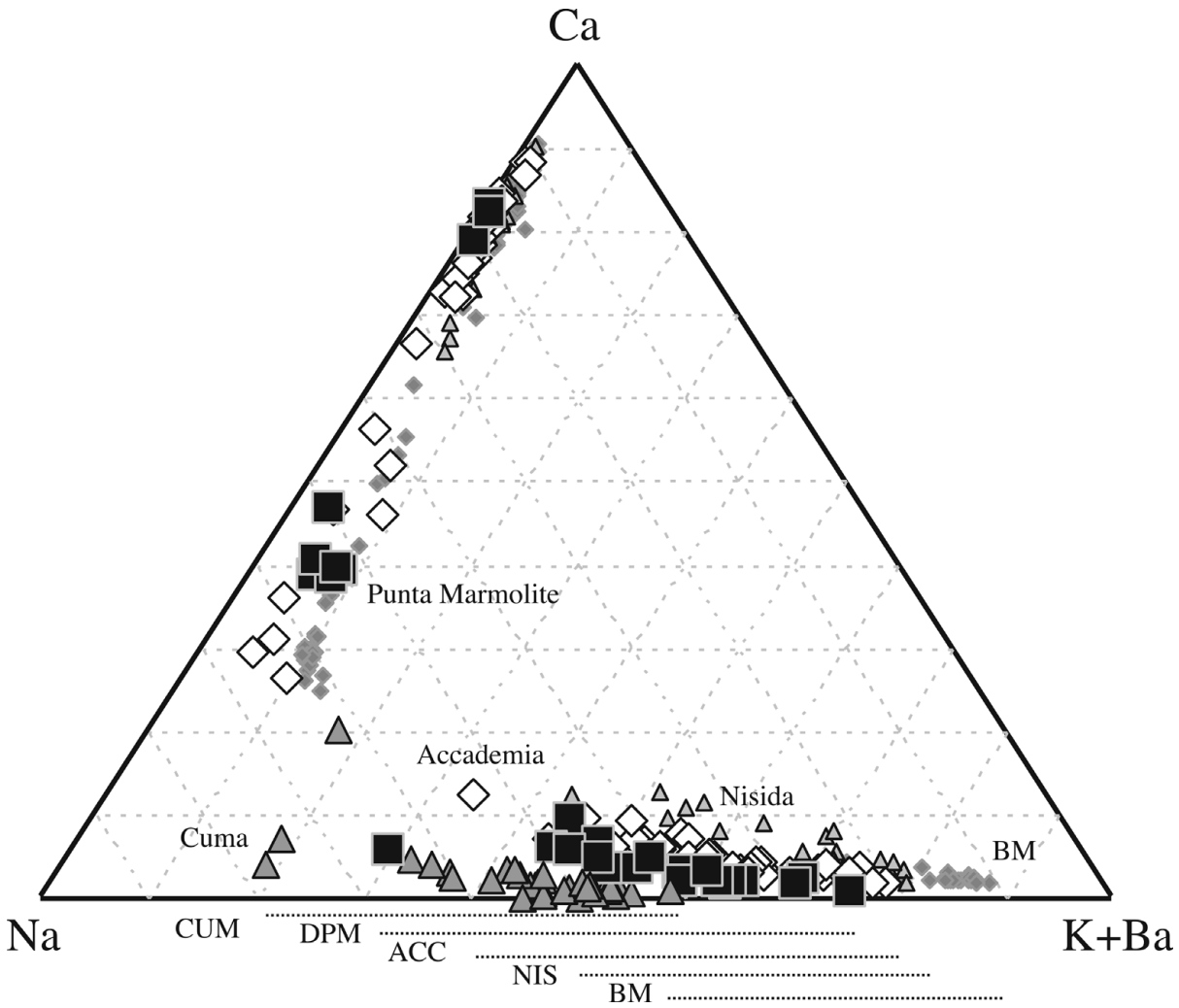

Figure 5. Ca–Na–K+Ba diagram for feldspar compositions. The feldspars of the Breccia Museo (grey diamonds) are from Fedele *et al*. (2008), those of Nisida are authors' unpublished data. The different ranges of alkali feldspar compositions are evidence of crystallization from differently evolved magmas, and that the increasing Na contents of the most potassic feldspars tend towards the minimum of the alkali feldspar loop ($Ab_{65}Or_{35}$), actually reached only in the Cuma samples.

exception of one relatively Ca-rich composition ($Ca_{20}Na_{62}K_{18}$; Fig. 5). A slightly more potassium- and calcium-rich sanidine ($Ca_{2–6}Na_{28–65}K_{75–29}$) is found in the Punta Marmolite samples rarely associated with very Ca-rich plagioclase ($Ca_{84–79}Na_{16–20}K_{0–1}$) with more sodic rims ($Ca_{47–38}Na_{49–55}K_{5–8}$). Sodium-rich pollucite ((Cs, Na)$AlSi_3O_8$) grains have been found in the groundmass of the Punta Marmolite dome (Fig. 2j; Table S1).

Ca-to-Na-rich plagioclase ($Ca_{87–26}Na_{11–64}K_{2–10}$) and K-rich sanidine ($Ca_{2–13}Na_{20–54}K_{78–34}$) are found as phenocrysts in the Accademia dome. Sr and Ba contents are relatively low throughout (up to 2 wt % SrO and 1.3 wt % BaO, respectively), as expected from the host-rock concentrations.

4.c. Sodalite, nepheline and analcime

Sodalite is the main feldspathoid of the Phlegrean rocks. It is idiomorphic in the Punta Marmolite samples, with a typical hexagonal shape, resembles analcime in other Phlegrean rocks (Fig. 2e, l) and typically occurs as an interstitial phase in the samples from the Cuma and Accademia domes. As usual, it shows very limited solid solution to the other volatile-rich feldspathoids, thus is almost devoid of K, Ca and SO_3 (see Melluso, Morra & Di Girolamo, 1996; Melluso, Morra & de' Gennaro, 2011).

Nepheline has been found in Punta Marmolite samples. It ranges in composition from $Ne_{79}Ks_{13}Sil_8$ to $Ne_{78}Ks_9Sil_{13}$ (end-members in wt %), displaying high Na/(Na + K) (= 0.87–0.91), relatively high silica excess and low Ca contents (0.6–1.5 wt % CaO; Table S1). Similar nephelines have been found in the Toppo S. Paolo phonolite, whereas the bulk of the Mt Vulture nephelines have a much lower silica excess than the Punta Marmolite compositions (Melluso, Morra & Di Girolamo, 1996; Melluso, Morra & de' Gennaro, 2011).

https://doi.org/10.1017/S0016756811000902 Published online by Cambridge University Press

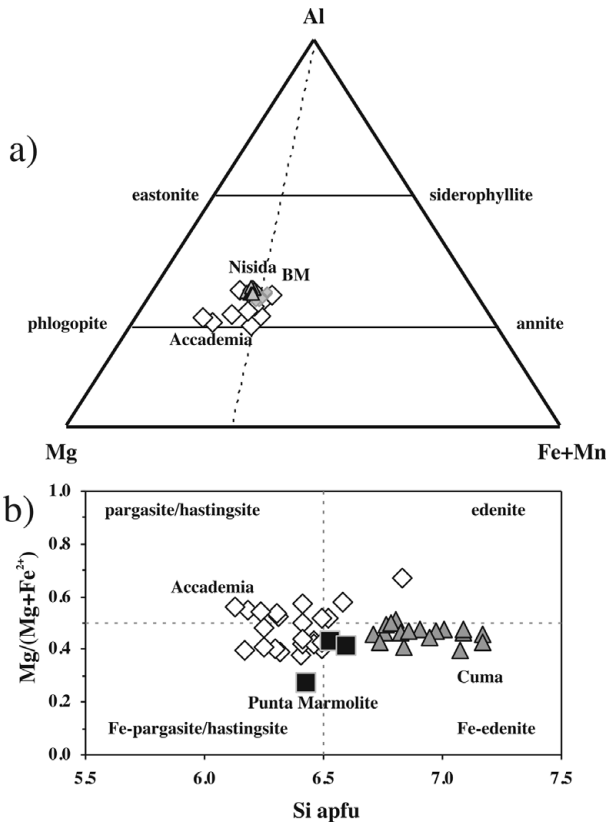

Figure 6. (a) Phlogopite and (b) amphibole classification diagrams. Phlogopite compositions of Breccia Museo (BM) are taken from Fedele *et al*. (2008). The phlogopite compositions of the Nisida tuff cone are authors' unpublished data.

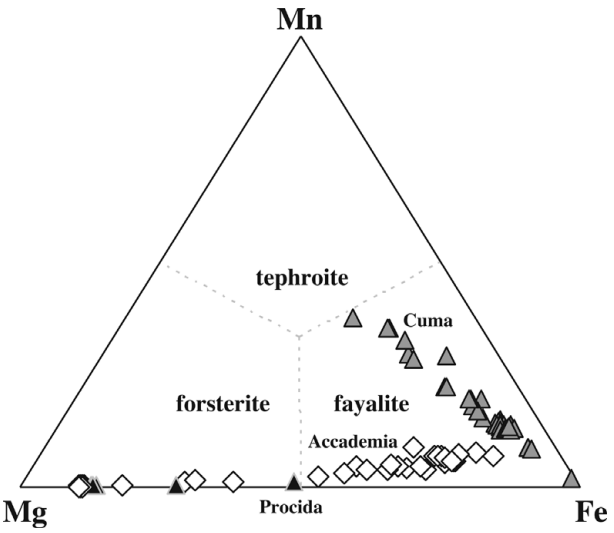

Figure 7. Fe–Mg–Mn diagram for the analysed olivine compositions. Olivine compositions of Procida (Solchiaro eruption) are unpublished data of the first author.

4.d. Amphibole and phlogopite

Brown-greenish amphibole is common in the groundmass of Cuma samples, is rare in the Punta Marmolite samples, but is typically found in the samples of the Accademia dome, both as the classical rim on clinopyroxene (Fig. 2j) and as a late-crystallized groundmass phase. The compositions are distinct, with pargasite, Fe-pargasite and Fe-pargasitic hornblende (with a few edenites) found in the Accademia samples, and Fe-edenite in the Cuma samples (Fig. 6). The rare amphibole in the Punta Marmolite dome is a ferro-edenitic to ferro-pargasitic hornblende (Table S1). The range of Mg nos is similar for the Cuma and Accademia samples (Mg no. = 40–51 at Cuma; Mg no. = 38–67 at Accademia) and slightly lower in the Punta Marmolite samples (Mg no. = 27–43). The TiO_2 content never exceeds 1.9 wt %, and MnO reaches similar values (up to 2.1 wt %; Table S1). No alkali amphiboles were positively identified: therefore, amphibole crystallized before the late-stage liquid reached peralkaline compositions.

Phlogopite is rare or absent in the Cuma and Punta Marmolite samples, and more common in the Accademia samples in the form of corroded phenocrysts and in glomeroporphyritic clusters with plagioclase, clinopyroxene and magnetite. It has a Mg no. from 64 to 74, F from 0.6 to 6.4 wt %, and moderate Ba and Ti contents (up to 1.2 wt % BaO and 5.5 wt % TiO_2, respectively; Table S1).

4.e. Olivine

Olivine of the Cuma samples is exclusively found as microlites in the groundmass, often in contact with aegirine (Fig. 2d), and ranges in composition from pure fayalite ($Mg_1Fe_{96}Ca_2Mn_2$, in atoms %) to tephroite-rich olivine ($Mg_{22}Fe_{40}Ca_2Mn_{37}$; Fig. 7). In the Accademia samples (e.g. OL2), idiomorphic, zoned olivine phenocrysts (Fig. 2k) range from $Mg_{89}Fe_{10}Ca_1Mn_0$ to $Mg_{61}Fe_{37}Ca_1Mn_1$, while groundmass microlites in samples OL1, OL2 and DAF1 range from $Mg_{45}Fe_{52}Ca_0Mn_2$ to $Mg_{12}Fe_{79}Ca_2Mn_7$, with a small compositional gap from the most to the least Mg-rich compositions, and with no resemblance to the olivine compositions found in the groundmass of the Cuma rocks. Olivine is absent in the Punta Marmolite dome (Table S1). The most Fe-rich olivines of the Cuma samples also carry small amounts of Zn (up to 0.5 wt % ZnO).

The Mg-rich crystals of the Accademia lava dome include chromiferous spinels (Fig. 2k and see next Section). In the groundmass, olivine matches the compositions found in evolved trachytic-rhyolitic magmas (see Ronga *et al*. 2010 for examples with similar compositional ranges).

4.f. Chromiferous spinel, magnetite and other spinels

Magnetite is the main Fe–Ti oxide in the Cuma and Punta Marmolite domes. The compositions are quite different, with the Cuma spinels showing the highest ulvöspinel content (62 mol % ulvöspinel, corresponding to 20 wt % TiO_2). Mn contents in magnetite reach relatively high values (4.5 wt % MnO). Additional manganoan gahnite (MnO = 12.8–13.7

https://doi.org/10.1017/S0016756811000902 Published online by Cambridge University Press

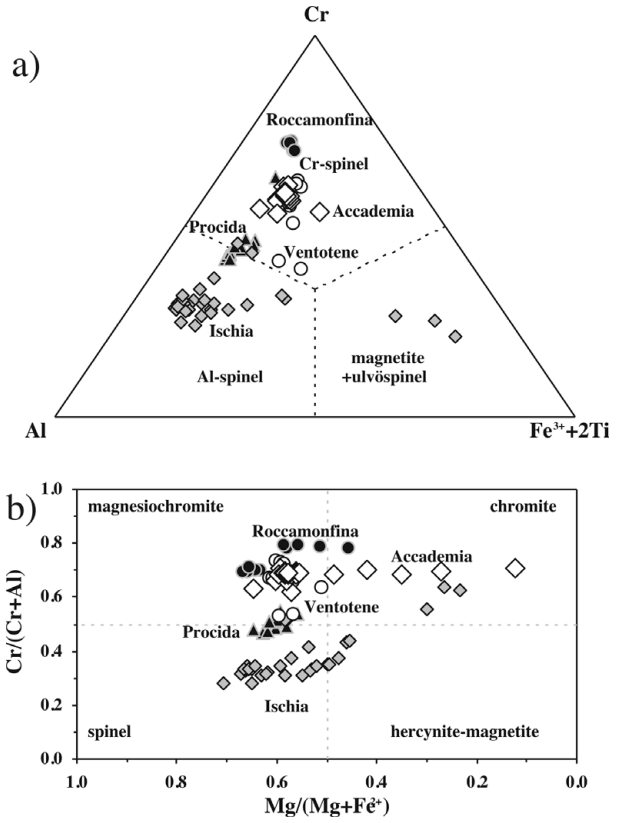

Figure 8. (a) Cr–Al–Fe^{3+} + 2Ti and (b) Mg/(Mg + Fe^{2+}) v. Cr/(Cr + Al) diagrams for the chromiferous spinel compositions of Accademia. Spinels from Ischia, Procida, Ventotene and Roccamonfina are taken from D'Antonio & Di Girolamo (1994), Di Girolamo *et al*. (1995) and L. Melluso & S. Conticelli, unpub. data.

wt %; ZnO = 28.6–29.2 wt %; Al_2O_3 = 57.3–60 wt %) has been found in the Cuma samples as an inclusion in altered magnetite (Fig. 2d) and other Mn-spinels in the Punta Marmolite samples (Table S1). In the Accademia samples, magnetite of the groundmass has TiO_2 up to15 wt % and MnO up to 3.6 wt %. No ilmenite was found.

Chromiferous spinel has been found in Mg-rich olivine phenocrysts and microphenocrysts of the Accademia dome (Fig. 2k). It ranges from magnesiochromite to chromite, with a significant range in Mg/(Mg + Fe^{2+}), from 0.12 to 0.65, and minor in Cr/(Cr + Al), from 0.62 to 0.71 (Fig. 8). The Ti concentration is low (0.5–1.5 wt % TiO_2; Table S1), as typical of spinels crystallized in primitive basalts and found in olivines with high forsterite content (see Melluso, de' Gennaro & Rocco, 2010; S. Conticelli & L. Melluso, unpub. data).

4.g. Baddeleyite, fluorite, pyrochlore, rosenbuschite, thorite, zircon and zirconolite

The three lava domes have small amounts of groundmass baddeleyite (ZrO_2), occasionally U-rich (1–3.7 wt % UO_2). In the Cuma samples, baddeleyite is accompanied by zircon. Pyrochlore ($(Ca,Na)_2Nb_2O_6(OH,F)$) is common in the Cuma rocks, and rare in the other outcrops. It is very rich in U (10.5–17.7 wt % UO_2), and almost devoid of Th (Table S1). A few Mn-rich compositions are also found. Fluorite (CaF_2) is another very common groundmass mineral, often inglobated by rosenbuschite in the Cuma dome. It is completely devoid of solid solutions to Na–Al or Sr fluorides (Table S1). Rosenbuschite, a typical Zr–F-rich disilicate ($(Ca,Na)_3(Zr,Ti)Si_2O_7(OH,F)_2$), is a featuring accessory phase in the groundmass of the Cuma dome. The composition is widely variable relative to reference compositions (e.g. Christiansen, Johnsen & Makovicky, 2003; Andersen *et al*. 2010), and has a high concentration of Na (7.6–12.5 wt % Na_2O), Mn (2.6–8.1 wt % MnO) and Fe (4–9.9 wt % FeO), widely variable Ca (7–25 wt % CaO) and low Ti (0.7–2.1 wt % TiO_2), at ZrO_2 ranging from 16.8 to 21.3 wt % and Nb_2O_5 from 1.7 to 3.7 wt % (Table S1). Fluorine varies from 5.6 to 8.4 wt %. Na and Ca have a marked negative correlation, and so is the relationship between Zr and Nb, and Ca and Fe, but the substitutions are certainly complex, given also the high concentration of Fe and Mn and the substantially unknown oxidation state of these two elements. The REE, Th and U contents are very low (Table S1). Zirconolite ($CaZrTi_2O_7$) has been found in the Accademia dome, sometimes as rims of baddeleyite. The composition has high Nb (10.3 wt % Nb_2O_5; Table S1). Thorite ($ThSiO_4$) has been found at Cuma.

We did not find titanite, which is the main Ti-rich mineral found in Phlegrean juvenile rocks and intrusive syenitic ejecta.

4.h. Apatite-britholite and monazite

Fluorapatite ($Ca_5(PO_4)_3(F,OH)$), almost systematically zoned to britholite ($REE_5(SiO_4)_3(OH,F)$; Fig. 2a, b), is a common mineral of all the samples of this study. The compositions vary from pure apatite, relatively poor in lanthanides, Th and U, to compositions very rich in a britholite component (e.g. SiO_2 = 20.5 wt %; P_2O_5 = 8.2 wt %; atomic $Si^*100/(Si + P)$ = 72–75), which carry notable concentrations of lanthanides, Th and U (Table S1; Fig. 9). The marked and systematic (core to rim) negative correlation between apatite and britholite components (Table S1; Fig. 9) suggest that inclusion of lanthanides, Th and U at the expense of Ca generates this substitution mechanism. Judging from Figure 9, it is possible that there is a compositional gap between apatite and britholite. A few crystals of britholite also contain locally significant amounts of arsenic (up to 7–18 wt % AsO_4), pointing to additional solid solution with P and Si involving johnbaumite and svabite end-members (nomenclature of Pasero *et al*. 2010). Fluorine decreases with increasing britholite components (from 5 wt % to nearly 0 wt %). Monazite (nominally $(La,Ce,Nd)PO_4$) has been found in the Cuma rocks (Table S1). It has La_2O_3, Ce_2O_3 and Nd_2O_3 reaching contents as high as 55–56 wt %, high Th (5–5.5 wt % ThO_2) and low Ca (0–3 wt % CaO).

https://doi.org/10.1017/S0016756811000902 Published online by Cambridge University Press

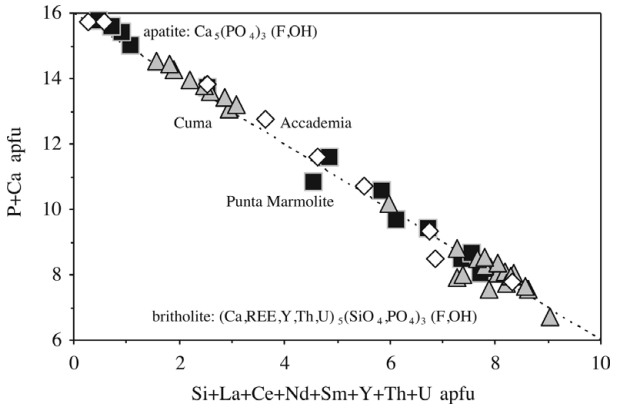

Figure 9. Apatite–britholite compositions as plotted in the Ca + P (apatite) v. Si + REE + U + Th (britholite) diagram (16 cations for 26 oxygens).

5. Discussion

5.a. Conditions of crystallization

The weakly peralkaline character of the most evolved rocks of the Phlegrean Fields was recognized long ago (e.g. Armienti *et al*. 1983; Di Girolamo *et al*. 1984; see also Poli *et al*. 1987 for the Ischian volcanic rocks), but no mineral assemblages typical of peralkaline products were identified; therefore, the evidence of a true peralkaline nature has previously been elusive. The Cuma rocks, having the most extreme mineral assemblages typical of peralkaline volcanic rocks, are among the most evolved compositions of the Phlegrean Fields, at roughly the same level as those of the AD 1538 Monte Nuovo eruption (Figs 3, 10) and more evolved than the most evolved compositions of the Campanian Ignimbrite (Melluso *et al*. 1995; Fedele *et al*. 2008). Mineral assemblages roughly similar to that of the Cuma dome were found in sanidinite facies 'syenitic' ejecta at Procida and Monte di Procida (see Mazzi & Munno 1983; Fedele *et al*. 2007; L. Melluso, unpub. data), but not yet in Phlegrean magmatic rocks. Zr-silicates of the wöhlerite group were described in trachytes of Ischia by Rittmann (1948).

In terms of classification (e.g. Sørensen, 1974, p. 22), the Cuma trachyphonolites are not peralkaline (having AI $\leq$ 1), but they have a groundmass assemblage made up of minerals typical of peralkaline undersaturated rocks, specifically peralkaline rocks with agpaitic affinity (i.e. having an AI > 1.2, with sodic pyroxenes or amphiboles, and Na–Ca–Zr–Ti silicates), as opposed to assemblages of typical miaskitic (e.g. with titanite $\pm$ zircon assemblages), non-peralkaline silica-undersaturated rocks. Trachytic/phonolitic magmas and intrusive equivalents (alkali and nepheline syenites) commonly cross the miaskitic/agpaitic crystallization stage (e.g. Larsen & Sørensen, 1987; Brotzu *et al*. 1997, 2007; Markl *et al*. 2001; Ridolfi *et al*. 2006; Bailey *et al*. 2006; Melluso *et al*. 2007; Andersen *et al*. 2010; Marks *et al*. 2011), so this high degree of evolution cannot be considered as unexpected in the Phlegrean Fields magmatism, particularly if we consider holocrystalline facies products, where the complete mineral assemblages can be easily studied.

The Punta Marmolite and Accademia domes have groundmass compositions with only a weak peralkaline trend (cf. the highly Fe-rich, but relatively Na-poor clinopyroxene compositions of the Punta Marmolite samples), and typical minerals indicating agpaitic affinity are lacking. The silica-undersaturated assemblage of Cuma, made up of anorthoclase, sodalite, Na-rich clinopyroxene and Zr-silicates, closely resembles the assemblages of the Ilimaussaq intrusion (see fig. 4a of Larsen & Sørensen, 1987; Markl *et al*. 2001; Bailey *et al*. 2006), with the main difference being the occurrence of F-bearing Ca–Zr-silicates (rosenbuschite) rather than Cl-bearing analogues (eudialyte and so on). In the Cuma lava dome, it appears that crystallization of sodalite scavenged substantial amounts of Cl from the melts, strongly increasing the F/Cl ratio and allowing subsequent stabilization of F-rich phases, including fluorite. After crystallization of sodalite, Cl-free feldspathoids, such as the nepheline of the Punta Marmolite, can crystallize. The presence of fluorite indicates the attainment of the maximum allowed fluorine fugacity, in the same way as sodalite indicates the maximum allowed chlorine fugacity (see Dolejs & Baker, 2004; Andersen *et al*. 2010). Lacking quantitative studies of the mineral assemblages found (and allowed) in similar rocks, the association fluorite–rosenbuschite–pyrochlore found at Cuma indicates relatively high activity of $Na_2Si_2O_5$ (peralkaline component) and HF, and relatively low H_2O (Andersen *et al*. 2010). Indeed, aegirine, the most typical indicator of peralkaline compositions, is one of the latest minerals to crystallize (see Fig. 2d). Nonetheless, the crystallization order of the various accessory phases in the Cuma samples, excluding favourable situations, cannot be established with certainty.

The position of the samples of this study in the nepheline–kalsilite–silica phase diagram is highly indicative. The Accademia dome latites plot close to the alkali feldspar join (as well the samples from the Nisida volcano; Fig. 10), whereas the Punta Marmolite and Cuma samples plot towards the phonolite minimum (reflecting increasing feldspathoid components), but without reaching it. Feldspar compositions become more sodic and thus migrate towards the minimum of the alkali feldspar loop, as typical of low temperature compositions of residual melt compositions worldwide (see Nash, Carmichael & Johnson, 1969). The Punta Marmolite rocks represent one of the rare cases in magmatic systems where nepheline, sanidine and sodalite co-crystallized (see the hypothetical phase diagram in Kogarko, Ryabchikov & Sørensen, 1974; see also Barker, 1976; Bailey *et al*. 2006; Andersen *et al*. 2010). High F (> 3000 ppm) and Cl (> 5000 ppm) are known in trachytic samples of the Phlegrean Fields (Ricci, 2000; Signorelli & Carroll, 2002 and references therein; this study). Furthermore, it is well known that

https://doi.org/10.1017/S0016756811000902 Published online by Cambridge University Press

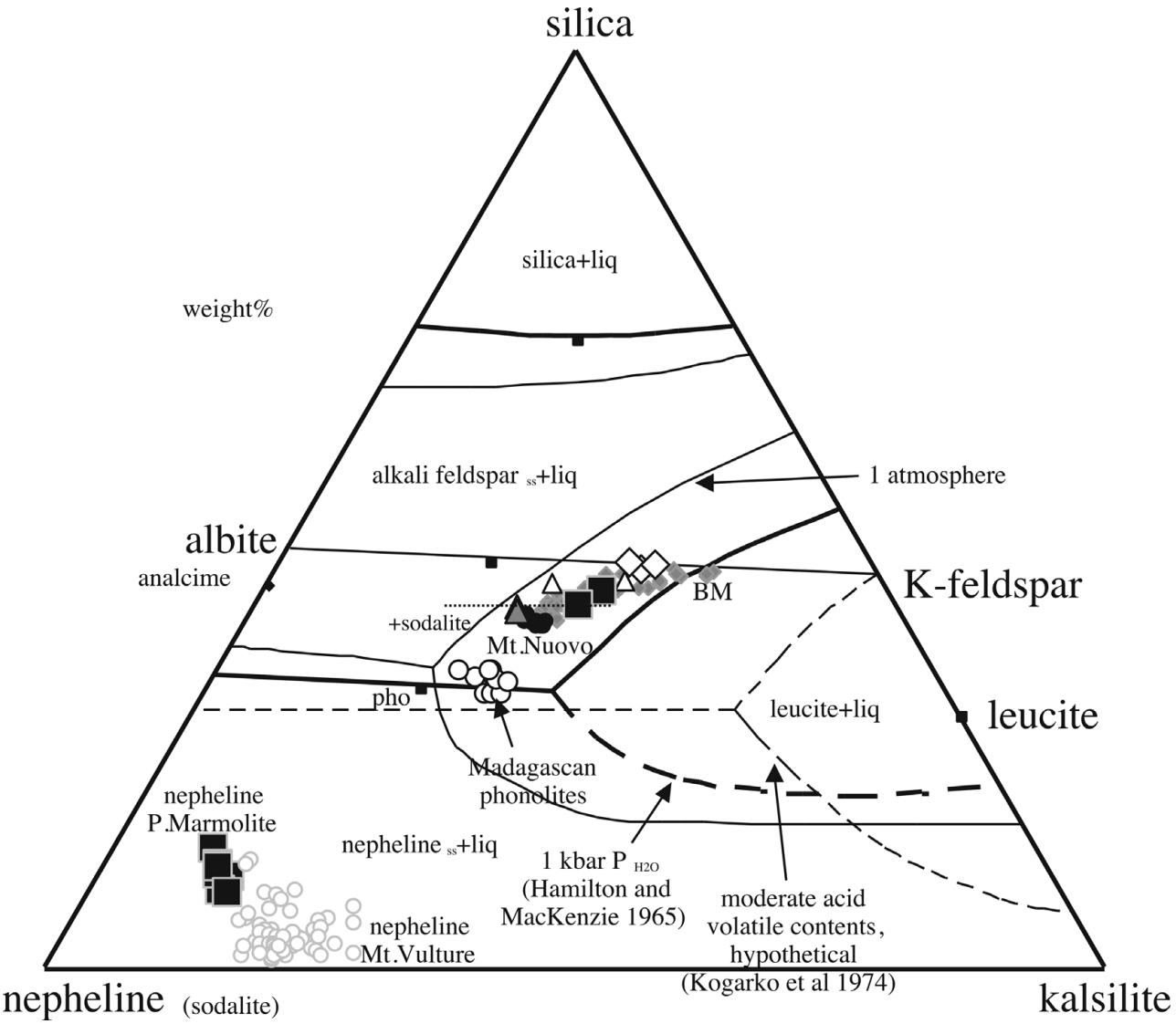

Figure 10. Nepheline compositions, bulk-rock compositions and reference nepheline–kalsilite–silica diagram at 1 atmosphere and 1 kbar P_{H2O} after Hamilton & MacKenzie (1965). Other inferred boundary lines are from Kogarko, Ryabchikov & Sørensen (1974). Data from D'Oriano *et al*. (2005; Monte Nuovo); Melluso *et al*. (2007; Madagascan phonolites); Fedele *et al*. (2008; Breccia Museo (BM)). The nephelines of Mt Vulture are also shown for comparison (data from Melluso, Morra & Di Girolamo, 1996; Melluso, Morra & de' Gennaro, in press). The inferred appearance of sodalite in the crystallization sequence is shown with a dashed line on the phase diagram.

fluorine has high solubility in depolymerized and silica-undersaturated magmas (e.g. Carroll & Webster, 1994; Dolejs & Baker, 2004; Mysen, Cody & Smith, 2004). Chlorine can have a lower, but roughly similar degree of solubility (see Signorelli & Carroll, 2002), as indicated by the occurrence of sodalite in the three domes, and even as phenocrysts in the Punta Marmolite samples. Therefore, the abundance of Cl (and F as well) in the Phlegrean (and Ischian) evolved magmas, testified by the occurrence of sodalite, affects the position of the minimum melt compositions, increasing the stability field of a feldspathoid such as sodalite at the expense of nepheline and alkali feldspar (see Sharp *et al*. 1989; Fig. 10). High F and Cl fugacity in the melts is well known to heavily shrink the leucite liquidus volume (see Kogarko, Ryabchikov & Sørensen, 1974; Fig. 10), and all these rocks plot within the leucite stability field in the nepheline–kalsilite–silica diagram at one atmosphere (Fig. 10). There is little doubt that all these domes crystallized their groundmass at conditions close to atmospheric pressure, but none of them has any trace of leucite. It is worth remembering that leucite also has a different morphology (rounded or pseudo-octagonal), compared to that typical of sodalite, and that leucite is never systematically hexagonal in shape, when idiomorphic. Sodalite is never a replacement phase, and is always interstitial to sanidine; on the other hand, it can be easily replaced by analcime, as it is observed, for instance, in the products of the Nisida tuff cone (Fig. 2l). We additionally note that hydrous minerals (amphibole and phlogopite) are rare in the Phlegrean rocks, including the holocrystalline facies.

https://doi.org/10.1017/S0016756811000902 Published online by Cambridge University Press

Therefore, the use of anhydrous or hydrous versions of the nepheline–kalsilite–silica phase diagram (see Arienzo *et al*. 2010) is only a very rough approximation of the actual crystallization conditions, as volatiles more soluble in magmas, like F and Cl, can more effectively influence the crystallization behaviour of the evolved Phlegrean magmas, also at depth, and these two elements are indeed present in significant amounts of the volatile budget of evolved trachytic magmas, as clearly shown in this and other papers. The appearance of sodalite in the mineral assemblages could be one of the several causes of the absence of genuine phonolites (i.e. evolved, low-Mg volcanic rocks with anorthoclase and feldspathoid phenocrysts, Fe-rich minerals, and bulk-rock SiO_2 around 55–56 wt %) at Phlegrean Fields, considering also that these volatile-rich melts are low-mass residues of slightly silica-undersaturated basaltic compositions, different from the Somma-Vesuvius phonolites, or typical (sodic) basanite–phonolite magmatic lineages (cf. typical phonolites shown in Fig. 10).

Olivines of the Cuma dome have by far the most Mn-rich fayalite compositions found in magmatic rocks of the Roman Province (see Melluso, Conticelli & de' Gennaro, 2010 for further Fe-rich groundmass olivines in other Roman Province rocks). The coexistence of these Fe^{2+}-rich olivines (± aenigmatite) with Fe^{3+}-rich aegirine (see Fig. 2d) is a rare and noteworthy feature (see Marks *et al*. 2011). Furthermore, Mg–Mn–Fe-olivines should form complete solid solutions (see Uchida, Kitamura & Imai, 1997), but the stability field of such high-Fe, high-Mn olivine is substantially unknown and, given that aegirine can crystallize also in reduced environments (e.g. Mitchell & Fareeduddin, 2009), clear links between mineral assemblages, composition of minerals, oxygen fugacity and silica activity still need much experimental work. The silica activity of some of the Phlegrean Fields trachyphonolites seems to be constrained between the baddeleyite–zircon and albite–nepheline equilibrium (see Barker, 2001), and may indicate an $a_{SiO2} < 0.6$–0.55 at 1100 °K. It cannot be excluded that the lack of zircon indicates a slightly lower silica activity, at least in the groundmass, but the well-known high solubility of zirconium in peralkaline melts has also to be taken into account. At any rate, the late-crystallized assemblage of the Cuma rocks shows evidence for the expected increasing degree of silica undersaturation.

5.b. The role of other accessory phases

High-silica and REE, low-Ca–P britholite is an extremely common (though highly underestimated) accessory mineral of the Italian potassic-ultrapotassic volcanic rocks (e.g. Melluso, Conticelli & de' Gennaro, 2010; Melluso, Morra & de' Gennaro, 2011 and unpub. data), and it occurs also in other volcanic rocks elsewhere (e.g. Ilimaussaq: Rønsbo, 2008; Olkaria: Macdonald *et al*. 2008; our unpub. data). Britholite is with no doubt the most important host for lanthanides, and, possibly, U and Th, of evolved holocrystalline volcanic rocks. The systematic occurrence of a zoned phosphate-silicophosphate in the three lava domes is interesting for at least two aspects: (1) the environment where apatite crystallized was increasingly poorer in P and Ca, and (2) the other included elements, particularly lanthanides, Th and U, were strongly incompatible in the early crystallized phases (feldspar, spinel, clinopyroxene and olivine), so they were heavily concentrated in residual melt fractions, and eventually fixed into the late-crystallized accessory phases. A direct evidence of such crystallization processes in the Phlegrean magmas is noted in the parallel patterns of the lanthanides, with the highest values found in the Cuma samples (Fig. 3c). This indicates no significant involvement of accessory phases in the fractional crystallization processes. Eu, Ba and Sr are low because they were scavenged by earlier feldspar fractionation (as an example, the cores of sanidine phenocrysts at Nisida reach 3 wt % BaO and 1.2 wt % SrO; authors' unpub. data; see the bright sanidine cores in the BSE image of Fig. 2l).

It is also interesting to note the variable partitioning behaviour among elements with generally similar geochemical behaviour (e.g. Th in monazite and thorite, U in pyrochlore and baddeleyite, U and Th in britholite, REE, Zr and Nb in various minerals), which still require compelling explanation.

5.c. High-temperature phases in trachytes: phenocrysts or xenocrysts?

Olivine with a high forsterite content ($Fo_{88–90}$) is commonly observed in primitive shoshonitic basalts of the nearby Procida island and in mafic shoshonitic inclusions at Ischia (Beccaluva, Di Girolamo & Serri, 1991; D'Antonio & Di Girolamo, 1994; Di Girolamo *et al*. 1995; our unpub. data). The same composition (Fo_{89}) cannot be expected in an evolved rock such as the Accademia lava dome. Indeed, the bulk-rock Mg nos of samples OL1 and OL2 are low (Mg no. = 44–48), and the bulk-rock MgO and Ni (and Cr) concentrations are so low that they cannot be in equilibrium with such a forsterite-rich olivine including chromite. Analogous reasoning can be inferred for plagioclase as calcic as An_{87}, Mg-rich diopside as is a $Ca_{48}Mg_{45}Fe_7$ composition (Mg no. = 88), and chromiferous spinel with Cr_2O_3 as high as 45–46 wt %. Therefore, all these phases must be considered as magmatic xenocrysts in any Phlegrean trachyte and latite (Fedele *et al*. 2009; cf. Fowler *et al*. 2007 for an alternative view). The crystallization of a Ca-rich plagioclase is even earlier than, or contemporaneous with, Mg-rich clinopyroxene, as again observed in mafic rocks of Procida and Ischia (see D'Antonio & Di Girolamo, 1994; Di Girolamo *et al*. 1995), thus demonstrating that calcic plagioclase cannot be a late-crystallized phase. Similar considerations can be made for the Ca-rich plagioclase sporadically found in Punta Marmolite samples, which testifies to

https://doi.org/10.1017/S0016756811000902 Published online by Cambridge University Press

recycling of phases derived from more mafic magma batches.

5.d. Relevance to the Phlegrean magmatism

The lava domes of this study allow inferences to be made on the evolution of the Phlegrean magmatic system. The samples from the Cuma dome give evidence of a substantially closed-system evolution process, such as: (1) weakly peralkaline agpaitic parageneses and compositions, indicating a prolonged differentiation history; (2) absence of high-temperature xenocrysts (such as those of the Accademia and Punta Marmolite domes); (3) absence of reversely zoned crystals, again suggesting that the evolving magmas did not experience significant interaction with less-evolved melts. The attainment of such extremely evolved compositions can be modelled by means of least-squares major element mass balance calculations (Table 2), performed following the method of Stormer & Nicholls (1978). Whole-rock and mineral compositions, used respectively for initial and final magma compositions and fractionated phases, are those reported in this work. The obtained results indicate that the transition from latite (sample OL1 from the Accademia lava dome) to trachyphonolite (DC2, Cuma dome) can be adequately modelled (i.e. with a ΣR^2 of 0.43–0.44; ΣR^2 = sum of square residuals) assuming ~ 89–92 % removal of an assemblage mainly made of alkali feldspar (46–47 %), plagioclase (27–29 %) and clinopyroxene (10–11 %), accompanied by olivine (3.4–5.7 %) and accessory magnetite or apatite + phlogopite. Similar results can be obtained by splitting the above transition in two steps (ΣR^2 = 0.18–0.36 and 0.26–0.45, respectively): (1) from latite to trachyte (DAF1, Accademia dome), implying 12–20 % removal of clinopyroxene and plagioclase (plus accessory olivine/phlogopite), and then (2) from trachyte to trachyphonolite, assuming 76–85 % removal of alkali feldspar (50–53 %), plagioclase (18–24 %), clinopyroxene (4–5 %) and accessory magnetite and olivine. The transition from Punta Marmolite to Cuma has been successfully modelled with *c.* 34 % removal of sanidine, plagioclase and mafic phases as accessories (Table 2). The results, together with the increasing Eu troughs from the least to the most evolved compositions (Fig. 3; Table 1) again point out the essential role of feldspar (first plagioclase and then alkali feldspar) removal in the formation and evolution of trachytic magmas (e.g. Melluso *et al*. 1995; Fedele *et al*. 2008, 2009). This transition towards the most evolved magmas took place at all the stages of activity (i.e. pre-CI, CI–NYT and post-CI) of the Phlegrean Fields, as widely documented (e.g. Armienti *et al*. 1983; Di Girolamo *et al*. 1984; Rosi & Sbrana, 1987; Villemant, 1988; Ghiara, 1989–1990; Beccaluva *et al*. 1990; Civetta *et al*. 1991, 1997; Scarpati, Cole & Perrotta, 1993; Melluso *et al*. 1995; Orsi *et al*. 1995; D'Antonio *et al*. 1999; de Vita *et al*. 1999; Pappalardo

Table 2. Major oxide mass balance calculations for the transition from Accademia to Cuma and Punta Marmolite lava dome samples

Transition	ol%	cpx%	plg%	Kfs%	mt%	phl%	ap%	*f*%	ΣR^2
latite (OL1)–trachyphonolite(DC2)	3.14	10.57	26.89	46.38	1.6				
	(Fo_{62})	($Di_{30}Wo_{48}Hd_{22}$)	($Ab_{60}Or_4An_{36}$)	($Ab_{20}Or_{78}An_2$)	(Usp 45%)			11.4	0.43
	5.70	9.89	29.32	47.25		0.09			
	(Fo_{40})	($Di_{30}Wo_{48}Hd_{22}$)	($Ab_{60}Or_4An_{36}$)	($Ab_{20}Or_{78}An_2$)		(Mg no. 0.65)	0.03	7.7	0.44
latite (OL1)–trachyte(DAF1)	1.48	7.08	8.38	3.29					
	(Fo_{62})	($Di_{36}Wo_{49}Hd_{15}$)	($Ab_{60}Or_4An_{36}$)	($Ab_{20}Or_{78}An_2$)				79.8	0.18
		7.55	3.74			0.88			
		($Di_{36}Wo_{49}Hd_{15}$)	($Ab_{41}Or_3An_{56}$)			(Mg no. 0.66)		87.8	0.36
trachyte(DAF1)–trachyphonolite(DC2)	0.86	5.03	17.82	49.81	2.29				
	(Fo_{62})	($Di_{30}Wo_{48}Hd22$)	($Ab_{60}Or_4An_{36}$)	($Ab_{20}Or_{78}An_2$)	(Usp 45%)			24.2	0.26
	2.47	3.91	23.79	53.06	1.57				
	(Fo_{40})	($Di_{30}Wo_{48}Hd_{22}$)	($Ab_{63}Or_6An_{31}$)	($Ab_{20}Or_{78}An_2$)	(Usp 45%)			15.2	0.45
trachyte(DAF1)–trachyte(DPM3)		5.35	16.05	41.8	1.68				
		($Di_{26}Wo_{48}Hd_{26}$)	($Ab_{63}Or_6An_{31}$)	($Ab_{20}Or_{78}An_2$)	(Usp 25%)			35.1	0.47
trachyte(DPM3)–trachyphonolite(DC2)	0.53	0.67	7.45	24.69	1.07				
	(Fo_{40})	($Di_{26}Wo_{48}Hd_{26}$)	($Ab_{45}Or_9An_{46}$)	($Ab_{20}Or_{78}An_2$)	(Usp 25%)			65.6	0.03

For each of the modellized transitions the wt % of subtracted olivine (ol%), clinopyroxene (cpx%), plagioclase (plg%), K-feldspar (Kfs%), magnetite (mt%), phlogopite (phl%) and apatite (ap%), the fraction of residual liquid (*f*%) and the sum of the square residuals (ΣR^2) are reported.

https://doi.org/10.1017/S0016756811000902 Published online by Cambridge University Press

et al. 1999, 2002; D'Oriano *et al*. 2005; Fedele *et al*. 2008; Arienzo *et al*. 2010).

Assuming a single magma chamber at least for the recent Phlegrean volcanic rocks, we are confident that the modelled transition from latite to trachyphonolite, as observed by comparing compositions of Accademia dome and Nisida tuff cone (3.9 ka) with those of Monte Nuovo (0.5 ka), took place in a closed system within a few thousand years. Although this is only a qualitative estimate, we note that these timescales are shorter (even allowing for a narrower differentiation step) than the $\sim$ 200 ka estimated on the basis of thermodynamic modelling for the production of the trachytic magmas of the Campanian Ignimbrite starting from a more primitive basaltic trachyandesite (latite) (Fowler *et al*. 2007).

The Accademia and, to a lesser extent, the Punta Marmolite lava domes are petrographically characterized by xenocrysts, testifying to open-system processes. The relatively abundant Accademia xenocrysts, clearly derived from primitive magmas, may have been picked up from a cumulitic layer in the shallow feeder system of the Phlegrean Fields or introduced into trachytic magma chambers by primitive magma recharge. The latter seems to be more reasonable, as the presence of a cumulitic (gabbroic/ultramafic?) layer at shallow depths in the Phlegrean area seems unlikely, given the negative buoyancy of basaltic magmas and their crystallization products (*sensu lato*), owing to their higher density with respect to wall rocks. It thus appears much more likely that sporadic batches of primitive magmas locally found favourable tectonic conditions that allowed them to reach the shallowest magma chambers, where they interacted with the residing volumes of evolved liquids. Therefore, olivine, chromite, plagioclase and clinopyroxene compositions of the Accademia dome record interaction of an evolved trachytic melt residing in a magma reservoir with a primitive, mantle-derived composition, as indicated by the relative proportion of 'trachytic' and 'basaltic' phenocrysts in the different facies and by the uniform trachytic texture and composition of the groundmass. This feature is also observed in the mineral composition of the nearby (and almost identical in age) Nisida tuff cone (e.g. Fig. 4), and in the Breccia Museo (CI) pyroclastic deposits as well (see Fedele *et al*. 2008, 2009). Di Girolamo *et al*. (1995) described blobs of very primitive basaltic compositions in Ischian trachytes, thus suggesting that open-system behaviour is a common feature of the Campanian volcanic rocks.

It is finally noted that the chemical composition of the chromiferous spinel found in the olivines of the Accademia dome does not overlap with the chromiferous spinel compositions found in the olivines at Procida (Solchiaro), recent lavas of Ischia (Zaro and Arso lava flows) and Roccamonfina and Ventotene island shoshonitic basalts and leucite-basanites (Fig. 8), clearly suggesting that the shoshonitic basalt magma batches of the volcanic fields in western Campania, from which those spinels grew, crystallized in independent reservoirs with independent crystallization histories.

Both closed-system and open-system evolution processes are evident in the magmatic history of the Phlegrean Fields, and this is observed in rocks erupted throughout its entire time span. This strongly argues in favour of a somewhat cyclic behaviour of the Phlegrean magmatic system, as also previously documented mainly on the basis of isotopic evidence (e.g. D'Antonio *et al*. 1999, 2007; Pappalardo *et al*. 1999, 2002; Di Renzo *et al*. 2011). This cyclic behaviour can be the consequence of a relatively random arrival of hot mafic magma from depth, recharging the magmatic reservoir(s) and triggering new eruptive periods.

6. Conclusions

The crystallization histories of three Phlegrean Fields lava domes show cooling of trachytic magma batches having different degrees of magmatic evolution in a closed-to-open magmatic system. Extreme closed-system fractional crystallization generated peralkaline compositions with appropriate mineral assemblages, such those found at Cuma. Closed-system fractional crystallization had the most important role in the magmatic evolution of the Phlegrean magmas, ultimately leading to Cl and F-rich trachyphonolites with peralkaline affinity, very poor in P, Sr and Ba and with mineral assemblages comprising anorthoclase, sodalite, aegirine, Mn–Fe-rich olivine, britholite, rosenbuschite, fluorite and other Zr-, Nb- and F-rich phases, thus reaching the agpaitic stage.

Open-system process are indicated by the occurrence of Ca-rich plagioclase, Mg-rich clinopyroxene, forsteritic olivine and chromiferous spinel in chemically evolved rocks. These phases crystallized in primitive, Mg-rich basalt compositions, rather than in the trachytic or latitic composition where they were found. The phases were introduced into the evolved compositions during magma chamber recharge, a possible trigger of the eruption.

Acknowledgements. We thank P. Cappelletti, S. Conticelli, D. Cosentino, C. Cucciniello, M. P. D'Albora and M. de' Gennaro for supplying samples, help in the field and laboratory work, for sharing unpublished data and for useful suggestions. Sergio Bravi is gratefully thanked for his skilled ability and patience in thin-section preparation. Initial versions of this manuscript benefitted from the useful comments and advice of Ray Macdonald and David Pyle. Two anonymous journal reviewers and Philip Leat provided further constructive comments and advice. Grants for this study were provided by Regione Campania (Legge Regionale n.5 to L. M.: Petrological study of the magmatic feeding systems of Somma-Vesuvius, Phlegrean Fields, and Ischia, similarities, differences and implications for the eruptive styles).

References

ANDERSEN, T., ERAMBERT, M, LARSEN, A. O. & SELBEKK, R. S. 2010. Petrology of nepheline syenite pegmatites in the Oslo Rift, Norway: zirconium silicate mineral assemblages as indicators of alkalinity and volatile fugacity in mildly agpaitic magmas. *Journal of Petrology* **51**, 2303–25.

ARIENZO, I., MORETTI, R., CIVETTA, L., ORSI, G. & PAPALE, P. 2010. The feeding system of Agnano-Monte Spina eruption (Campi Flegrei, Italy): dragging the past into present activity and future scenarios. *Chemical Geology* **270**, 135–47.

ARMIENTI, P., BARBERI, F., BIZOUARD, H., CLOCCHIATTI, R., INNOCENTI, F., METRICH, N., ROSI, M. & SBRANA, A. 1983. The Phlegrean Fields: magma evolution within a shallow chamber. *Journal of Volcanology and Geothermal Research* **17**, 289–311.

AVANZINELLI, R., LUSTRINO, M., MATTEI, M., MELLUSO, L. & CONTICELLI, S. 2009. Potassic and ultrapotassic magmatism in the circum-Tyrrhenian region: significance of carbonated pelitic vs. pelitic sediment recycling at destructive plate margins. *Lithos* **113**, 213–27.

BAILEY, J. C., SØRENSEN, H., ANDERSEN, T., KOGARKO, L. N. & ROSE-HANSEN, J. 2006. On the origin of microrhythmic layering in arfvedsonite lujavrite from the Ilimaussaq alkaline complex, south Greenland. *Lithos* **91**, 301–18.

BARKER, D. S. 1976. Phase relations in the system $NaAlSiO_4$-SiO_2-NaCl-H_2O at 400°-800°C and 1 kilobar, and petrologic implications. *Journal of Geology* **84**, 97–106.

BARKER, D. S. 2001. Calculated silica activities in carbonatitic liquids. *Contributions to Mineralogy and Petrology* **141**, 704–9.

BECCALUVA, L., COLTORTI, M., Di GIROLAMO, P., MELLUSO, L., MILANI, L., MORRA, V. & SIENA, F. 2002. Petrogenesis and evolution of Mt. Vulture alkaline volcanism (Southern Italy). *Mineralogy and Petrology* **74**, 277–97.

BECCALUVA, L., DI GIROLAMO, P., MORRA, V. & SIENA, F. 1990. Phlegrean Fields volcanism revisited: a critical re-examination of deep eruptive systems and magma evolutionary processes. *Neues Jahrbuch Geologische Paläontologische Monatshefte* h.**5**, 257–71.

BECCALUVA, L., Di GIROLAMO, P. & SERRI, G. 1991. Petrogenesis and tectonic setting of the Roman Volcanic Province, Italy. *Lithos* **26**, 191–221.

BOYNTON, W. V. 1984. Cosmochemistry of the rare earth elements: meteorite studies. In *Rare Earth Element Geochemistry* (ed. P. Henderson), pp. 63–114. Amsterdam: Elsevier.

BROTZU, P., GOMES, C. B., MELLUSO, L., MORBIDELLI, L., MORRA, V. & RUBERTI, E. 1997. Petrogenesis of coexisting SiO_2-undersaturated to SiO_2-oversaturated felsic igneous rocks: the alkaline complex of Itatiaia, southeastern Brazil. *Lithos* **40**, 133–56.

BROTZU, P., MELLUSO, L., BENNIO, L., GOMES, C. B., LUSTRINO, M., MORBIDELLI, L., MORRA, V., RUBERTI, E., TASSINARI, C. C. G. & D'ANTONIO, M. 2007. Petrogenesis of the Cenozoic potassic alkaline complex of Morro de São João, southeastern Brazil. *Journal of South American Earth Sciences* **24**, 93–115.

CARROLL, M. R. & WEBSTER, J. D. 1994. Solubilities of sulfur, noble gases, nitrogen, chlorine and fluorine in magmas. *Reviews of Mineralogy* **30**, 231–79.

CASSIGNOL, C. & GILLOT, P. Y. 1982. Range and effectiveness of unspiked potassium-argon dating: experimental groundwork and application. In *Numerical Dating in Stratigraphy* (ed. G. S. Odin), pp. 159–69. New York: Wiley.

CHRISTIANSEN, C. C., JOHNSEN, O. & MAKOVICKY, E. 2003. Crystal chemistry of the rosenbuschite group. *The Canadian Mineralogist* **41**, 1203–24.

CIVETTA, L., CARLUCCIO, E., INNOCENTI, F., SBRANA, A. & TADDEUCCI, G. 1991. Magma chamber evolution under the Phlegrean Fields during the last 10 ka: trace element and isotope data. *European Journal of Mineralogy* **3**, 415–28.

CIVETTA, L., ORSI, G., PAPPALARDO, L., FISHER, R. V., HEIKEN, G. & ORT, M. 1997. Geochemical zoning, mingling, eruptive dynamics and depositional processes – the Campanian Ignimbrite, Campi Flegrei caldera, Italy. *Journal of Volcanology and Geothermal Research* **75**, 183–219.

D'ANTONIO, M. 2011. Lithology of the basement underlying the Campi Flegrei caldera: volcanological and petrological constraints. *Journal of Volcanology and Geothermal Research* **200**, 91–8.

D'ANTONIO, M., CIVETTA, L. & DI GIROLAMO, P. 1999. Mantle source heterogeneity in the Campanian Region (South Italy) as inferred from geochemical and isotopic features of mafic volcanic rocks with shoshonitic affinity. *Mineralogy and Petrology* **67**, 163–92.

D'ANTONIO, M., CIVETTA, L., ORSI, G., PAPPALARDO, L., PIOCHI, M., CARANDENTE, A., DE VITA, S., DI VITO, M. A. & ISAIA, R. 1999. The present state of the magmatic system of the Phlegrean Fields caldera based on a reconstruction of its behavior in the past 12 ka. *Journal of Volcanology and Geothermal Research* **91**, 247–68.

D'ANTONIO, M. & DI GIROLAMO, P. 1994. Petrological and geochemical study of mafic shoshonitic volcanics from Procida-Vivara and Ventotene Islands. *Acta Volcanologica* **5**, 69–80.

D'ANTONIO, M., TONARINI, S., ARIENZO, I., CIVETTA, L. & DI RENZO, V. 2007. Components and processes in the magma genesis of the Phlegrean Volcanic District, southern Italy. In *Cenozoic Volcanism in the Mediterranean Area* (eds L. Beccaluva, G. Bianchini & M. Wilson), pp. 203–20. Geological Society of America Special Paper no. 418.

DEINO, A. L., ORSI, G., DE VITA, S. & PIOCHI, M. 2004. The age of the Neapolitan Yellow Tuff caldera-forming eruption (Campi Flegrei caldera – Italy) assessed by $^{40}Ar/^{39}Ar$ dating method. *Journal of Volcanology and Geothermal Research* **133**, 157–70.

DE LA ROCHE, H., LETERRIER, P., GRANDCLAUDE, P. & MARCHAL, E. 1980. A classification of volcanic and plutonic rocks using R_1-R_2 diagram and major element analyses. Its relationships with current nomenclature. *Chemical Geology* **29**, 183–210.

DE VITA, S., ORSI, G., CIVETTA, L., CARANDENTE, A., D'ANTONIO, M., DEINO, A., DI CESARE, T., DI VITO, M. A., FISHER, R. V., ISAIA, R., MAROTTA, E., NECCO, A., ORT, M., PAPPALARDO, L., PIOCHI, M. & SOUTHON, J. 1999. The Agnano-Monte Spina eruption (4100 years BP) in the restless Campi Flegrei caldera (Italy). *Journal of Volcanology and Geothermal Research* **91**, 269–301.

DE VIVO, B., ROLANDI, G., GANS, P. B., CALVERT, A. T., BOHRSON, W. A., SPERA, F. J. & BELKIN, H. E. 2001. New constraints on the pyroclastic eruptive history of the Campanian volcanic Plain (Italy). *Mineralogy and Petrology* **73**, 47–65.

DI GIROLAMO, P. 1970. Differenziazione gravitativa e curve isochimiche nella "Ignimbrite Campana". *Rendiconti Società Italiana di Mineralogia e Petrologia* **26**, 3–44.

DI GIROLAMO, P., GHIARA, M. R., LIRER, L., MUNNO, R., ROLANDI, G. & STANZIONE, D. 1984. Vulcanologia e

https://doi.org/10.1017/S0016756811000902 Published online by Cambridge University Press

petrologia dei Campi Flegrei. *Bollettino della Società Geologica Italiana* **103**, 349–413.

Di Girolamo, P., Melluso, L., Morra, V. & Secchi, F. A. G. 1995. Evidence of interaction between mafic and intermediate magmas in the youngest activity phase of activity at Ischia Island. *Periodico di Mineralogia* **64**, 393–411.

Di Renzo, V., Arienzo, I., Civetta, L., D'Antonio, M., Tonarini, S., Di Vito, M. A. & Orsi, G. 2011. The magmatic feeding system of the Campi Flegrei caldera: architecture and temporal evolution. *Chemical Geology* **281**, 227–41.

Dolejs, D. & Baker, D. R. 2004. Thermodynamic analysis of the system Na_2O-K_2O-CaO-Al_2O_3-SiO_2-H_2O-F_2O_{-1}: stability of fluorine-bearing minerals in felsic igneous suites. *Contributions to Mineralogy and Petrology* **146**, 762–78.

D'Oriano, C., Poggianti, E., Bertagnini, A., Cioni, R., Landi, P., Polacci, M. & Rosi, M. 2005. Changes in eruptive style during the A.D. 1538 Monte Nuovo eruption (Phlegrean Fields, Italy): the role of syn-eruptive crystallization. *Bulletin of Volcanology* **67**, 601–21.

Fedele, L., Insinga, D. D., Calvert, A. T., Morra, V., Perrotta, A. & Scarpati, C. 2011. $^{40}Ar/^{39}Ar$ dating of tuff vents in the Campi Flegrei caldera (southern Italy): Toward a new chronostratigraphic reconstruction of the Holocene volcanic activity. *Bulletin of Volcanology*, published online 5 May 2011. doi:10.1007/s00445-011-0478-8.

Fedele, L., Scarpati, C., Lanphere, M., Melluso, L., Morra, V., Perrotta, A. & Ricci, G. 2008. The Breccia Museo formation, Phlegrean Fields, southern Italy: geochronology, chemostratigraphy and relationship with the Campanian Ignimbrite eruption. *Bulletin of Volcanology* **70**, 1189–219.

Fedele, L., Tarzia, M., Belkin, H. E., De Vivo, B., Lima, A. & Lowenstern, J. B. 2007. Magmatic-hydrothermal fluid interaction and mineralization in alkali syenite nodules from the Breccia Museo pyroclastic deposit, Naples, Italy. In *Volcanism in the Campania Plain: Vesuvius, Campi Flegrei and Ignimbrites* (ed. B. De Vivo), pp. 125–61. Developments in Volcanology no. 9. Amsterdam: Elsevier

Fedele, L., Zanetti, A., Morra, V., Lustrino, M., Melluso, L. & Vannucci, R. 2009. Clinopyroxene/liquid trace element partitioning in natural trachyte–trachyphonolite systems: insights from Phlegrean Fields (southern Italy). *Contributions to Mineralogy and Petrology* **158**, 337–56.

Fowler, S. J., Spera, F. J., Bohrson, W. A., Belkin, H. E. & De Vivo, B. 2007. Phase equilibria on the chemical and physical evolution of the Campanian Ignimbrite. *Journal of Petrology* **48**, 459–93.

Ghiara, M. R. 1989–90. Studio evolutivo del sistema magmatico flegreo negli ultimi 10 ka. *Bollettino della Società dei Naturalisti in Napoli* **98–99**, 41–70.

Hamilton, D. L. & MacKenzie, W. S. 1965. Phase equilibrium studies in the system $NaAlSiO_4$-$KAlSiO_4$-SiO_2-H_2O. *Mineralogical Magazine* **34**, 214–31.

Insinga, D. D., Calvert, A. T., Lanphere, M., Morra, V., Perrotta, A., Sacchi, M., Scarpati, C., Saburomaru, J. & Fedele, L. 2006. The Late-Holocene evolution of the southwestern sector of Campi Flegrei as inferred by stratigraphy, petrochemistry and $^{40}Ar/^{39}Ar$ dating. In *Volcanism in the Campania Plain: Vesuvius, Campi Flegrei and Ignimbrites*. (ed. B. De Vivo), pp. 97–125. Developments in Volcanology no. 9. Amsterdam: Elsevier.

Isaia, R., Marianelli, P. & Sbrana, A. 2009. Caldera unrest prior to intense volcanism in Campi Flegrei (Italy) at 4.0 ka B.P.: implications for caldera dynamics and future eruptive scenarios. *Geophysical Research Letters* **36**, L21303, doi:10.1029/2009GL040513, 6 pp.

Kogarko, L. N., Ryabchikov, I. D. & Sørensen, H. 1974. Liquid fractionation. In *Alkaline Rocks* (ed. H. Sørensen), pp. 488–500. New York: Wiley.

Larsen, L .M. & Sørensen, H. 1987. The Ilimaussaq intrusion – progressive crystallization and formation of layering in an agpaitic magma. In *Alkaline Igneous Rocks* (eds G. Fitton & B. G. J. Upton), pp. 473–88. Geological Society of London, Special Publication no. 30.

Lyubetskaya, T. & Korenaga, J. 2007. Chemical composition of Earth's primitive mantle and its variance: 1. Methods and results. *Journal of Geophysical Research* **112**, B03211, doi: 10.1019/2005JB004223, 21 pp.

Macdonald, R., Baginski, B., Belkin, H. E., Dzierzanowski, P. & Jezak, L. 2008. REE partitioning between apatite and melt in a peralkaline volcanic suite, Kenya Rift Valley. *Mineralogical Magazine* **72**, 1147–61.

Macdonald, R., Baginski, B., Leat, P. T., White, J. C. & Dzierzanowski, P. 2011. Mineral stability in peralkaline silicic rocks: information from trachytes of the Menengai volcano, Kenya. *Lithos* **125**, 553–68.

Markl, G., Marks, M., Schwinn, G. & Sommer, H. 2001. Phase equilibrium constraints on intensive crystallization parameters of the Ilimaussaq complex, south Greenland. *Journal of Petrology* **42**, 2231–58.

Marks, M., Hettmann, K., Schilling, J., Frost, B. R. & Markl, G. 2011. The mineralogical diversity of alkaline igneous rocks: critical factors for the transition from miaskitic to agpaitic phase assemblages. *Journal of Petrology* **52**, 439–55.

Mazzi, F. & Munno, R. 1983. Calciobetafite (new mineral of the pyrochlore group) and related minerals from Phlegrean Fields, Italy; crystal structures of polymignyte and zirkelite: comparison with pyrochlore and zirconolite. *American Mineralogist* **68**, 262–76.

Melluso, L., Conticelli, S. & de' Gennaro, R. 2010. Kirschsteinite in the Capo di Bove melilite leucitite lava (cecilite), Alban Hills, Italy. *Mineralogical Magazine* **74**, 887–902.

Melluso, L., de' Gennaro, R. & Rocco, I. 2010. Compositional variations of chromiferous spinel in Mg-rich rocks of the Deccan Traps, India. *Journal of Earth System Science* **119**, 343–63.

Melluso, L., Morra, V. & de' Gennaro, R. 2011. Coexisting Ba-feldspar and melilite in a melafoidite lava of Mt. Vulture, Italy: role of volatiles and alkaline earths in bridging a petrological incompatibility. *The Canadian Mineralogist* **49**, 983–1000.

Melluso, L., Morra, V. & Di Girolamo, P. 1996. The Mt. Vulture volcanic complex (Italy): evidence for distinct parental magmas and for residual melts with melilite. *Mineralogy and Petrology* **56**, 226–50.

Melluso, L., Morra, V., Perrotta, A., Scarpati, C. & Adabbo, M. 1995. The eruption of The Breccia Museo (Phlegrean Fields, Italy): fractional crystallization processes in a shallow, zoned magma chamber and implications for the eruptive dynamics. *Journal of Volcanology and Geothermal Research* **68**, 325–39.

Melluso, L., Morra, V., Riziky, H., Veloson, J., Lustrino, M., Del Gatto, L. & Modeste, V. 2007.

Petrogenesis of a basanite-tephrite-phonolite volcanic suite in the Bobaomby (Cap d'Ambre) peninsula, northern Madagascar. *Journal of African Earth Sciences* **49**, 29–42.

MITCHELL, R. H. & FAREEDUDDIN 2009. Mineralogy of peralkaline lamproites from the Raniganj coalfield, India. *Mineralogical Magazine* **73**, 457–77.

MORRA, V., CALCATERRA, D., CAPPELLETTI, P., COLELLA, A., FEDELE, L., DE' GENNARO, R., LANGELLA, A., MERCURIO, M. & DE' GENNARO, M. 2010. Urban geology: relationships between geological setting and architectural heritage of the Neapolitan area. In *Geology of Italy, Journal of the Virtual Explorer*, vol. 36, paper 26 (eds M. Beltrando, A. Peccerillo, M. Mattei, S. Conticelli & C. Doglioni), doi: 10.3809/jvirtex.2010.00261.

MYSEN, B. O., CODY, G. D. & SMITH, A. 2004. Solubility mechanism of fluorine in peralkaline and metaaluminous silicate glasses and in melts to magmatic temperatures. *Geochimica et Cosmochimica Acta* **68**, 2745–69.

NASH, W. P., CARMICHAEL, I. S. E. & JOHNSON, R. W. 1969. The mineralogy and petrology of Mt. Suswa, Kenya. *Journal of Petrology* **10**, 409–39.

ORSI, G., CIVETTA, L., D'ANTONIO, M., DI GIROLAMO, P. & PIOCHI, M. 1995. Step-filling and development of a three-layer magma chamber: the NYT case history. *Journal of Volcanology and Geothermal Research* **67**, 291–312.

ORSI, G., DI VITO, M. A., SELVA, J. & MARZOCCHI, W. 2009. Long-term forecast of eruption style and size at Campi Flegrei caldera (Italy). *Earth and Planetary Science Letters* **287**, 265–76.

PABST, S., WÖRNER, G., CIVETTA, L. & TESORO, R. 2008. Magma chamber evolution prior to the Campanian Ignimbrite and Neapolitan Yellow Tuff eruptions (Phlegrean Fields, Italy). *Bulletin of Volcanology* **70**, 961–76.

PAPPALARDO, L., CIVETTA, L., D'ANTONIO, M., DEINO, A., DI VITO, M. A., ORSI, G., CARANDENTE, A., DE VITA, S., ISAIA, R. & PIOCHI, M. 1999. Chemical and Sr-isotopic evolution of the Phlegrean magmatic system before the Campanian Ignimbrite and the Neapolitan Yellow Tuff eruptions. *Journal of Volcanology and Geothermal Research* **91**, 141–66.

PAPPALARDO, L., PIOCHI, M., D'ANTONIO, M., CIVETTA, L. & PETRINI, R. 2002. Evidence for multi-stage magmatic evolution during the past 60 kyr at Campi Flegrei (Italy) deduced from Sr, Nd and Pb isotope data. *Journal of Petrology* **43**, 1415–34.

PASERO, M., KAMPF, A. R., FERRARIS, C., PEKOV, I. V., RAKOVAN, J. & WHITE, T. J. 2010. Nomenclature of the apatite supergroup minerals. *European Journal of Mineralogy*, **22**, 163–79.

PERROTTA, A., SCARPATI, C., LUONGO, G. & MORRA, V. 2006. The Campi Flegrei caldera boundary in the city of Naples. In *Volcanism in the Campania Plain: Vesuvius, Campi Flegrei and Ignimbrites*. (ed. B. De Vivo), pp. 85–96. Developments in Volcanology no. 9. Amsterdam: Elsevier.

POLI, S., CHIESA, S., GILLOT, P. Y., GREGNANIN, A. & GUICHARD, F. 1987. Chemistry versus time in the volcanic complex of Ischia (Gulf of Naples, Italy): evidence of successive magmatic cycles. *Contributions to Mineralogy and Petrology* **95**, 322–35.

RICCI, G. 2000. *Il distretto vulcanico dei Campi Flegrei: petrologia e geochimica dei depositi di breccia e dei depositi piroclastici associati*. Ph.D. thesis, Università di Napoli, 95 pp. Published thesis.

RIDOLFI, F., RENZULLI, A., MACDONALD, R. & UPTON, B. G. J. 2006. Peralkaline syenite autoliths from Kilombe volcano, Kenya Rift Valley: evidence for subvolcanic interaction with carbonatitic fluids. *Lithos* **91**, 373–92.

RITTMANN, A. 1948. Origine e differenziazione del magma ischitano. *Schweizerische Mineralogische Petrographische Mitteilungen* **28**, 643–98.

RONGA, F., LUSTRINO, M., MARZOLI, A. & MELLUSO, L. 2010. Petrogenesis of a basalt-comendite-pantellerite rock suite: the Boseti volcanic complex, Main Ethiopian Rift. *Mineralogy and Petrology* **98**, 227–43.

RØNSBO, J. G. 2008. Apatite in the Ilimaussaq alkaline complex: occurrence, zonation and compositional variation. *Lithos* **106**, 71–82.

ROSI, M. & SBRANA, A. 1987. The Phlegrean Fields. *C.N.R. Quaderni de "La ricerca scientifica"* **114**, vol. 10, 175 pp.

SCARPATI, C., COLE, P. & PERROTTA, A. 1993. The Neapolitan Yellow Tuff – a large volume multiphase eruption from Campi Flegrei, Southern Italy. *Bulletin of Volcanology* **55**, 343–56.

SHARP, Z. D., HELFFRICH, G. R., BOHLEN, S. R. & ESSENE, E. J. 1989. The stability of sodalite in the system $NaAlSiO_4$-NaCl. *Geochimica et Cosmochimica Acta* **53**, 1943–54.

SIGNORELLI, S. & CARROLL, M. R. 2002. Experimental study of Cl solubility in hydrous alkaline melts: constraints on the theoretical maximum amount of Cl in trachytic and phonolitic melts. *Contributions to Mineralogy and Petrology* **143**, 209–18.

SØRENSEN, H. 1974. *The Alkaline Rocks*. London: John Wiley and Sons, 622 pp.

STORMER, J. C. & NICHOLLS, J. 1978. XLFrac: a program for interactive testing of magmatic differentiation models. *Computers and Geosciences* **4**, 143–59.

UCHIDA, E, KITAMURA, Y. & IMAI, N. 1997. Mixing properties of Fe-Mn-Mg olivine solid solution determined experimentally by ion exchange method. *Journal of Mineralogy, Petrology and Economic Geology* **92**, 142–53.

VILARDO, G., TERRANOVA, C., BRONZINO, G., GIORDANO, S., VENTURA, G., ALESSIO, G., GABRIELE, M., MAINOLFI, R., PAGLIUCA, E. & VENERUSO, M. 2001. SISCam: Sistema Informativo Sismotettonico della Regione Campania. Laboratorio di Geomatica e Cartografia INGV-OV.

VILLEMANT, B. 1988. Trace element evolution in the Phlegrean Fields (central Italy): fractional crystallization and selective enrichment. *Contributions to Mineralogy and Petrology* **98**, 169–83.

WHITE, J. C., REN, M. & PARKER, D. F. 2005. Variation in mineralogy, temperature and oxygen fugacity in a suite of strongly peralkaline lavas and tuffs, Pantelleria, Italy. *The Canadian Mineralogist* **43**, 1331–47.